EPIGENETIC REGULATION OF SLIT-ROBO PATHWAY IN HEPATOCELLULAR CARCINOMA

A THESIS SUBMITTED TO
THE DEPARTMENT OF MOLECULAR BIOLOGY AND GENETICS
AND THE INSTITUTE OF ENGINEERING AND SCIENCE OF
BILKENT UNIVERSITY
IN PARTIAL FULFILLMENT OF THE REQUIREMENTS FOR
THE DEGREE OF MASTER OF SCIENCE

BY FATİH SEMERCİ

JULY 2009

TO MY PARENTS & MY BROTHER,

GÜNER – AHMET&ORHAN SEMERCİ

FOR THEIR LOVE AND SUPPORT

I certify that I have read this thesis and that in my opinion it is fully adequate, in scope, and in quality, as a thesis for the degree of Master of Science.

_____

Assist.Prof. Dr.Tamer Yağcı

I certify that I have read this thesis and that in my opinion it is fully adequate, in scope, and in quality, as a thesis for the degree of Master of Science.

_____

Assoc.Prof. Dr.Hilal Özdağ

I certify that I have read this thesis and that in my opinion it is fully adequate, in scope, and in quality, as a thesis for the degree of Master of Science.

_____

Assist.Prof. Dr.Özlen Konu

Approved for the Institute of Engineering and Science

_____

Prof. Dr. Mehmet Baray

Director of the Institute of Engineering and Science

ABSTRACT

EPIGENETIC REGULATION OF SLIT-ROBO PATHWAY IN HEPATOCELLULAR CARCINOMA

Fatih Semerci

MSc, in Molecular Biology and Genetics

Supervisor: Assist. Prof Tamer Yağcı

July, 2009 52 pages

Hepatocellular carcinoma is an aggressive, chemotherapy-resistant cancer and the prognosis of affected patients is very poor. Therefore, unraveling molecular components of hepatocarcinogenesis not only leads to the improvement of diagnostic and prognostic tools but also may reveal novel therapeutic targets. We previously defined the differential expression of *SLIT-ROBO* genes in HCC. To explore the mechanisms of the inactivation of these genes, we analyzed the hypermetylation of *SLIT1*, *SLIT2*, *ROBO2* and *ROBO3* genes in a group of HCC cell lines consisting of four high-AFP expressing well-differentiated (HUH7, Hep3B, PLC/PRF5 and HepG2) and low-AFP expressing poorly-differentiated cell lines (Focus, SKHep1, Snu387 and Snu423). We first demonstrated that the transcription of all studied genes can be rescued upon treatment of cell lines with 5-Aza-2'-deoxycytidine (5-Aza-dC). Next, we analyzed the methylation of *SLIT-ROBO* genes by methylation specific PCR. All genes were found to be at least partially methylated, except *ROBO3*, which displayed a heavily methylated pattern. *in silico* analyses of the 5' upstream sequence of *ROBO2* gene revealed a putative promoter region, an enhancer in the first intron and a CpG island. Methylation –specific PCR amplification of *ROBO2* by using primers selected from this CpG island supports the potential of this region as a gene regulatory site. Therefore, it is worthy to extend the methylation analyses of SLIT-ROBO pathway in HCC patients. Furthermore, mechanistic studies on ROBO3, which was shown to counteract the overexpressed ROBO1 effects may shed light into the role of ROBO3/ROBO1 axis and the potential of *ROBO3* as a tumor suppressor gene in HCC.

ÖZET

SLIT-ROBO YOLAĞININ HEPATOSELLÜLER KARSİNOMADA EPİGENETİK DÜZENLENMESİ

Fatih Semerci
Moleküler Biyoloji ve Genetik Yüksek Lisansı
Tez Yöneticisi: Yrd.Doç. Dr. Tamer Yağcı
Temmuz 2009, 52 Sayfa

Hepatoselüler karsinoma kemoterapiye dayanıklı, saldırgan ve kötü prognozla seyreden bir kanser türüdür. Bu yüzden HCC'nin ilerlemesinde etkisi olan moleküler bileşenlerinin ortaya çıkarılması sadece teşhis ve takip araçlarının iyileşmesine katkıda bulunmakla kalmayıp, yeni tedavi hedefi olabilecek moleküllerin bulunmasına da olanak sağlayabilir. Daha önce grubumuz tarafından *SLIT-ROBO* genlerinin hepatoselüler karsinomada farklı ifade örüntülerine sahip oldukları gösterildi. Bu genlerin etkisizleştirilmesinde rol alan mekanizmalarına ait detayları öğrenebilmek için *SLIT1, SLIT3, ROBO2* ve *ROBO3* genlerinin aşırı metillenme durumlarını 4 adet AFP ifadesi yüksek- iyi farklılaşmış (Huh7, Hep3B, PLC/PRF5 ve HepG2) ve 4 adet AFP ifadesi düşük- az farklılaşmış (SKHep1, FOCUS, Snu387 ve Snu423) karaciğer kanseri hücre hattında araştırdık. İlk olarak, araştırılan bütün genlerin ifadelerini 5-Aza-dC kullanılarak arttırılabileceğini gösterdik. Daha sonra, *SLIT-ROBO* genlerinin metillenme durumlarını metilasyona özel PCR reaksiyonu ile araştırdık. Araştırılan bütün genlerin en azından kısmi olarak metillenmiş oldukları, buna ek olarak da *ROBO3* geninin aşırı metillendiğini gösterdik. *in-silico* araştıma sonuçları *ROBO2* geninin 5' ucunun yukarısında yer alan bölgelerin potansiyel bir CpG adacığı, birinci intron içerisinde bir yükseltici, ve bir promotör bölge içerdiğini ortaya çıkardı. Bu CpG adacığına ait primerler kullanılarak yapılan PCR reaksiyonları bu bölgenin bir gen düzenleyici alan olduğunu destekledi. Dolayısıyla, SLIT- ROBO yolağının metilasyon analizlerinin HCC hastalarında da araştırmak yerinde olacaktır. Bunun yanında aşırı ifade edilen *ROBO1'*e zıt bir etki gösteren *ROBO3* geniyle yapılacak mekanistik çalışmalar *ROBO3/ROBO1* ekseninin rolünü aydınlatabilecek ve *ROBO3*'ün HCC'de bir tümör baskılayıcı gen olma potansiyeline ışık tutabilecektir.

ACKNOWLEDGEMENTS

It is a pleasure for me to thank the many people who made this thesis possible…

First and foremost, I would like to thank my thesis advisor Assist. Prof Tamer Yağcı for his supervision and guidance throughout this study. I am grateful for his patience, motivation, enthusiasm, and immense knowledge in molecular biology that, taken together, make him a great mentor.

I am really very lucky for meeting M. Ender Avcı who was my second advisor. He was very good teacher and I learned him a lot about the laboratory techniques. He has provided assistance in numerous ways during my experiments. Not to mention that he has been a great friend outside the laboratory.

I want to thank also to Dr. Hani Alotaibi, for sharing his experience in cloning and providing the vectors for this study.

I have been very happy to be a member of Bilkent MBG family. It would be very difficult to find such a lovely people in such a peaceful environment. I am very grateful to all my friends for whom I need a chapter to mention all. Nevertheless, my special "big thanks" go to Muammer Üçal, Ahmet Raşit Öztürk, Erdem Erikçi, Kutay Karatepe, Tamer Kahraman, Onur Kaya, Ceyhan Ceran, Ceren Sucularlı, Şerif Şentürk, Tolga Acun and Sinan Gültekin for their sincere friendship.

Also I want to thank all MBG supervisors Doç. Dr. Ali Güre ,Dr. Özlen Konu, Dr. Uygar Tazebay, Doç. Dr. Işık Yuluğ, Prof. Dr. Tayfun Özçelik, Dr. İhsan Gürsel, Dr. Cengiz Yakıcıer , Dr. Can Akçalı, Dr. Rengül Çetin-Atalay, Dr. Mehmet Öztürk for knowledge and experience they shared through my undergraduate and graduate years.

Last but not least, I wish to thank my parents and my brother. It is impossible to express my endless love and thanks to my family. I will forever grateful to them. I dedicate this thesis to them…

TABLE OF Contents

LIST OF FIGURES

LIST OF TABLES

ABBREVIATIONS

Amp	ampicillin
bp	Base Pairs
BSA	Bovine serum albumin
cDNA	Complementary DNA
Ct	Cycle Threshold
ddH2O	Double distilled water
DEPC	Diethylpyrocarbonate
DMEM	Dulbecco's Modified Eagle's Medium
DMSO	Dimethyl Sulfoxide
DNA	Deoxyribonucleic Acid
dNTP	Deoxyribonucleotide triphosphate
ds	Double strand
dsDNA	double-stranded DNA
EDTA	ethylenediaminetetraacetic acid
EtBr	Ethidium Bromide
FBS	Fetal Bovine Serum
GAPDH	glyceraldehyde-3-phosphate dehydrogenase
HBV	Hepatitis B Virus
HCC	Hepatocellular Carcinoma
HCV	Hepatitis C Virus
HDAC	histone deacetylase
LB	Luria-Bertani media
µg	Microgram
mg	Miligram
min	Minute
µl	Microliter
ml	Mililiter
µM	Micromolar
mM	Milimolar
mRNA	Messenger RNA
NaCl	Sodium Chloride
Oligo(dT)	Oligodeoxythymidylic acid
PBS	Phosphate Buffered Saline

PCR	Polymerase Chain Reaction
pmol	Picomole
PTEN	Phosphatase and Tensin homolog
qRT-PCR	Quantitative real time RT-PCR
RNA	Ribonucleic acid
Rpm	Revolutions Per Minute
RT PCR	Reverse Transcription PCR
Sec	Second
TAE	Tris-Acetate-EDTA buffer
Tm	Melting Temperature
Tris	Tris (Hydroxymethyl)- Methylamine
UV	Ultraviolet
5-Aza-dC	5-Aza-2’-deoxycytidine

CHAPTER 1 INTRODUCTION:

1.1 Hepatocellular Carcinoma:

The liver is the largest internal organ of the body. The physiological functions of liver can be summarized as follows: 1) Bile production and excretion 2) Excretion of bilirubin, cholesterol, hormones and drugs 3) Metabolism of proteins, fats and carbohydrates 4) Storage of glycogen, vitamins and minerals 5) Enzyme activation 6) Plasma protein (albumin and globulin) synthesis. 7) Blood detoxification and purification.

Hepatocellular Carcinoma (HCC) is the most frequent primary liver cancer. It is the fifth most common cancer world-wide and causes approximately 600,000 deaths per year (Llovet JM. et al., 2003). Hepatocarcinogenesis nearly always develops in the setting of chronic hepatitis or cirrhosis; conditions in which many hepatocytes are killed and inflammatory cells invade the liver and the connective tissue (Thorgeirsson SS and Grisham GW. et al., 2002). Chronic exposure to aflatoxin B1 and infection with hepatitis B virus, hepatitis C virus are responsible about 80% of all HCC in humans (Bosch FX. Et al., 1999). TGF-alpha and IGF-2 are the growth factors that are activated in response to hepatitis, infection with hepatitis B or C. This situation leads to increased proliferation of the cells with impaired G1/S checkpoint. Although this increased rate of proliferation is balanced by the loss of hepatocytes through apoptosis, it also results in the production of monoclonal populations of dysplastic hepatocytes (Thorgeirsson SS and Grisham GW. et al., 2002). During the preneoplastic stage, that may take 10 to 30 years to develop, additional changes occur like increased chromosomal abnormalities, loss of tumor suppressors, decreased expression of EGR1 and C/EBPα, and increased expression of FOXM1b. At later stages, increased expression of TGF-β is thought to be one of the main reasons of increased angiogenesis and metastasis (Greenbaum LE.et al., 2004).

1.2 CpG Methylation:

DNA methylation and other histone modifications are the key processes of the epigenetic regulation of the genome and they have crucial roles in the control of gene activity and nuclear architecture. Most widely studied epigenetic modification in humans is the CpG methylation. Presence of methylated cytosines in the genomic DNA is related to the chromosomal condensation, X inactivation, chromosome stabilization, genomic imprinting, and tissue specific silencing of the gene expression. This modification has a major role in the cell differentiation process of mammalian embryogenesis (Reik W., et al.,2001; Bacola. et

al.,1999) Potentially methylable CpG dinucleotides are not randomly distributed in the genome. They are condensed in the regions called CpG islands, which are mainly located in the gene regulatory sequences at 5' end region of the most genes (Esteller M., et al., 2007). In normal cells these regions are generally unmethylated and allow the transcription of genes in the presence of transcription factors. Contrary to this, repetitive genomic sequences are heavily methylated. The latter process has an important role in the protection of the chromosomal integrity by preventing chromosomal instability, translocations and gene disruption through the reactivation of endoparasitic sequences. (Esteller M., 2005; Walsh C.P., et al., 1998)

The methylation of mammalian genomic DNA is catalyzed by DNA methyltransferases (DNMTs) (**Figure 1.1**). DNMTs can be divided into two groups: Maintenance and de novo DNMTs. While maintenance DNMT1 binds methyl groups to the hemimethylated DNA during replication, de novo DNMT3A and DNMT3B add methyl groups to CpG dinucleotides of unmethylated DNA (Das P.M. et al., 2004).

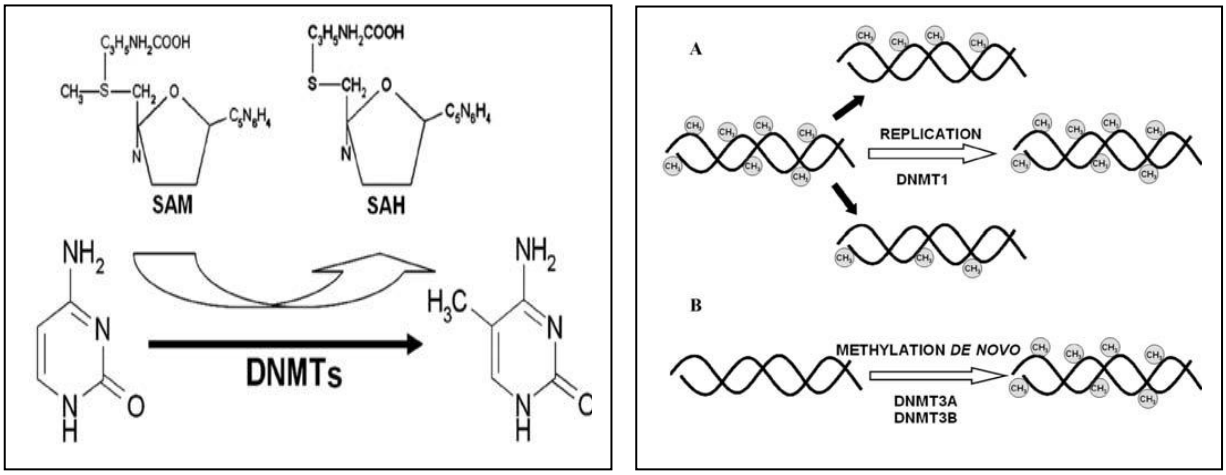

Figure 1.1 Methylation of cytosine within CpG dinucleotides is catalyzed by DNMTs. S-adenosylmethionine (SAM) donates methyl groups and is converted to S-adenosylhomocysteine (SAH).
Maintenance (A) and *de novo* DNMTs (B) methylate DNA. DNMT1 binds methyl groups to the hemimethylated DNA during replication, whereas DNMT3A and DNMT3B can add methyl groups to CpG dinucleotides of unmethylated DNA. (Luczak, M. W et al., 2006)

Presence of m^5CpG dinucleotides in DNA sequence directly inhibits transcription or recruits proteins that specifically recognize methylated DNA and initiate remodeling of euchromatin into heterochromatin structure. This euchromatin to heterochromatin transition contains the formation of the nuclease-resistant chromatin, methyl-CpG- binding proteins.

Methylated DNA recruits m^5CpG- binding domain (MBD) proteins MeCP1 and MeCP2 that bind specifically to methylated DNA in whole genome and form barriers against the binding of the transcription factors to the promoters. MeCP1 represses heavily methylated regions (promoters containing more than 10 m^5CpG dinucleotides), whereas MeCP2 can control the transcription of genes by binding to the single CpG dinucleotides that are symmetrically located in opposite DNA strands (Hendrich B, et al., 1998). Also, DNMTs are associated with histone deacetlyases (HDACs), histone methyltransferases (HMTs), HP1 which are key regulators of histone modification.(Wade, P. A. et al., 2001; Wang. Y. et al., 2004). Moreover DNMT3B additionally recruits the ATP dependent chromatin remodeling enzyme hSHF2H, which is involved in the heterochromatin formation. (Geiman TM, et al., 2004)

Methylation of CpG islands and then recruitment of the HDACS and other histone modifying enzymes is not the unique mechanism for epigenetic regulation of gene expression. Sometimes, histone modifications may favor or block the DNA methylation. In the fungus *Neurospora,* it has been shown that the ability to methylate histone Lys9 is required for DNA methylation (Jackson J. P., et al., 2002). This evidence suggests that local methylation of Lys9 may provide a signal for the methylation of the CpG islands in the close proximity. Also in different pathways, histone acetylation at promoters can lead to inhibition of DNA methylation (Mutskov V. J., et al., 2002).

1.2.1 Cancer and DNA Methylation:

Development of cancer may arise from either inherited mutations in the germ line cells or from changes in the DNA sequences of somatic cells during life. In turn, these sequence based changes either cause the activation of the protooncogenes or decrease the activity of the tumor suppressor genes. Additional to the sequence based mutations; epigenetic changes may also favor the development of cancer. Hyper/hypo-methylation of the promoter or the first exon of the cancer related genes is one of the common changes in the tumor cell genome. These epigenetic changes mimic the effect of the sequence based mutations in the tumor suppressor genes and protooncogenes.

1.2.1.1 Role of Hypomethylation of in Cancer Development:

Global hypomethylation of genomic DNA is a common feature of tumor cells and results in the overexpression of the protooncogenes, growth factors and genes related to invasion and metastasis (Szyf M, et al., 2004). For example, the expression of urokinase plasminogen activator (PLAU), heparanase, calcium binding protein (S100A4) and insulin-like growth factor 2 (IGF2), all known for their important role in the invasion and metastasis

of the tumors, is induced by hypomethylation (Senolt L. et al., 2006; Pakneshan P. et al.,2005).

Besides the protooncogenes, hypomethylation of retrotransposons also contribute to the progression of cancer by destabilization of the genome. This destabilization occurs via the insertional mutagenesis and recombination between non-allelic repeats (Jagodzinski P. P., et al., 2006). Heavy methylation of CpG islands in LINEs (Long interspersed nuclear elements) is a host defense against retrotransposon activation (Bestor. T. H., et al. 2000). Hypomethylation of LINEs was observed in colon cancer and chronic lymphatic leukemia(J. I. Goodman., et al, 2003).

Reasons of this global hypomethylation in malignant cell transformation are not clear. One hypothesis to explain this situation states that there is a complete or partial deficiency of numerous enzymes involved in methyl transport at the cellular level (Steele, W., C. Allegrucci, et al. 2005). But this hypothesis is not enough to explain the simultaneous hypermethylation of tumor suppressor genes promoter. Some findings suggest that overexpression of catalytic inactive variants of DNMT3B may shield CpG dinucleotides from active DNMTs (Weisenberger DJ et al., 2004).

1.2.1.2 Role of Hypermethylation of Tumor Suppressor Genes in Cancer Development:

In many cancer types there has been a significant correlation between the protein biosynthesis of DNMT1, DNMT3B and hypermethylation of CpG islands that are located in the promoter regions of CDKN2A (cyclin dependent kinase inhibitor 2A), CDKN2B, CDH1 (E-cadherin), MLH1(mismatch repair gene), RB1 (retinoblastoma 1), TIMP3 (TIMP metallopeptidase inhibitor 3), BRCA1, PTEN, TP53. (Table 1.1)

Tumor Suppressor Gene	Related Cancer	Reference
CDKN2A	Lymphoma	Herman J. G. et al., 1995.
CDKN2B	Leukemia	Melki JR. et al., 1999.
CDH1	Breast, Prostate,Colorectal	Darwanto A., et al., 2003. Graff JR., et al., 1995.
BRCA1	Breast, ovarian	Esteller M., et al., 2000
PTEN	Colorectal	Goel A., et al., 2004
MLH1	Colon	Veigl ML., et al., 1998
RB1	Retinoblastoma	Stirzaker C., et al., 1997
TIMP3	Colon, renal, brain	Bachman KE., et al., 1999
TP53	leukemia	Agirre X., et al., 2003

1.3 SLIT-ROBO Family:

It has always been a big challenge to understand how so many neurons are connected to each other to form functional circuits in a precise manner. This problem has been divided into several distinct but interdependent developmental processes: neuronal identity specification, polarization of neurons, initialization of axonal and dendritic outgrowth, navigation of axons and dendrites towards their targets, and formation of the synaptic contacts (Dickson and Gilestro et al., 2004). These complex series of events constitute a major obstacle in understanding axonal outgrowth. However, guidance of commissural axons in both vertebrates and *Drosophila* by Slit(s) and their Robo family receptors offers us a good model to understand the basic steps in the axon patterning.

1.3.1 Role of SLIT ROBO in the Guidance of Commissural Axons:

Commissural neurons are born in the dorsal spinal cord and their axons are drawn to the midline by chemoattractant proteins netrin and sonic hedgehog, which emanate from the ventral midline. (Charron et al. 2003, Kennedy et al. 1994, Serafini et al. 1994) After crossing the midline, axons turn to contralateral side and continue to grow right alongside of the floor plate. (**Figure 1.2**) SLIT and ROBO family members act as repulsive cues in this process and prevent axons from recrossing the ventral midline.

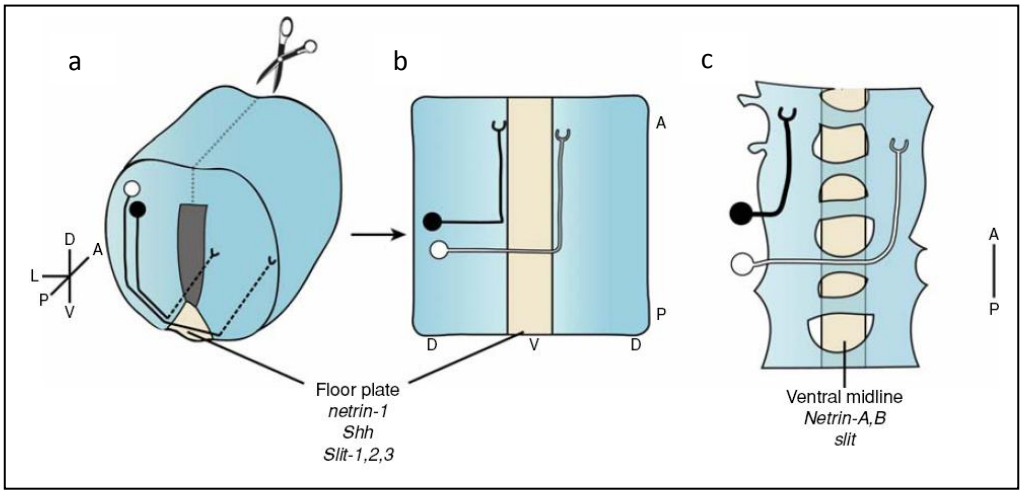

***Figure 1.2*:** (a) Spinal cord section from E 12.5 mouse embryo (b) "Open book" preparation, obtained by dissecting the spinal cord along the dashed line indicated in A. (c) Dorsal view of two segments of the ventral nerve cord, showing examples of intersegmental commissural (*white*) and ipsilateral (*black*) neurons. A, anterior; P, posterior; D, dorsal; V, ventral; L, lateral (Dickson and Gilestro et al., 2004)

1.3.1.1 SLITs:

The *Slit* gene encodes a 190 kDa protein in the secreted form and is produced by the midline cells (Rothberg JM et al. 1988, 1990). Its mutant form was identified in the classic genetic screen for embryonic patterning (Nüsslein- Volhard et al., 1984) and commissural axon path finding defects (Hummel et al., 1999) in *Drosophila*. Further genetic (Battye R. et al. 1999; Kidd T. et al., 1999) and biochemical (Brose K. et al., 1999; Li HS. et al., 1999) studies revealed the role of *Slit* as the ligand of *Robo*. Mammals have three slit genes (*Slit-1 Slit-2, and Slit-3*) which are expressed by the midline cells as their homologue in *Drosophila* (Brose K. et al., 1999; Holmes GP. et al., 1998; Itoh A. et al., 1998; Li HS. et al.,1999; Yuan W. et al., 1999b). Disruption of all three *Slit* genes in mice leads to abnormalities in the axon crossing through the midline or completely stalls the crossing (Long H.et al., 2004). Also the studies in *C. Elegans* showed that SLT-1 (Slit homologue in *C. Elegans*) is expressed at high levels in anterior epidermis and embryonic expression of that gene provides anterior-posterior guidance information to migrating neurons (Hao JC. et al., 2001). All of these works indicate that *Slit* proteins has a conserved role as a repellent guidance cues for commissural axons. (**Figure 1.3**)

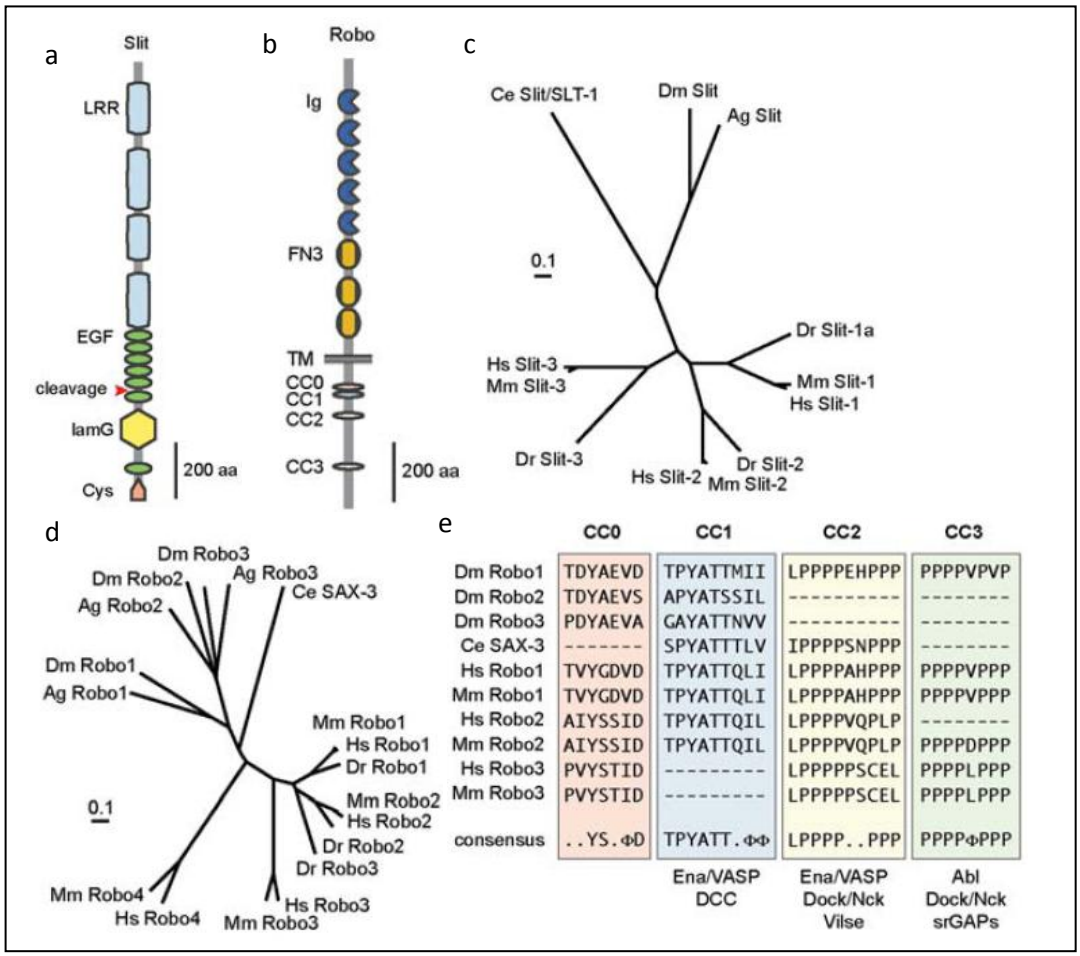

Figure 1.3: Species abbreviations used: Ag, *Anopheles gambiae*; Ce, *Caenorhabditis elegans*; Dm, *Drosophila melanogaster*; Dr, *Danio rerio*; Hs, *Homo sapiens*; Mm, *Mus musculus*. (a) Slit domain organization. Abbreviations used: aa, amino acids; LRR, leucine-rich repeat; EGF, epidermal growth factor–like repeat; lamG, laminin G domain; Cys, cysteine-rich domain. arrow head indicates cleavage site in vertebrates. (b) Robo domain organization Ig, immunoglobulin-like domain; FN3, fibronectin type 3 domain; TM, transmembrane region; CC0-3, conserved cytoplasmic motifs. (c) Phylogenetic analysis of Slit family proteins. (d) Phylogenetic analysis of Robo family, prepared by only using the extracellular sequences only. (e) Alignment of selected CC motifs with consensus sequences and binding partners. (Dickson and Gilestro et al., 2004)

Slit proteins share a common domain structure which consists of a series of four leucine rich repeats, seven to nine epidermal growth factors (EGF) like domains, a laminin G domain and a C terminal cysteine-rich domain (**Figure 1.3**). Most of the *Slits* are cleaved within the EGF-like region by unknown proteases (Brose K. et al., 1999; Wang KH. et al., 1999). It was proved that these proteolytic fragments of Slit protein have distinct activities in vitro like repelling of the olfactory bulb axons in collagen gel. This repelling also leads to olfactory bulb growth cones to collapse (Nguyen Ba-Charvet et al., 2001).

1.3.1.2 ROBOs:

Identification of *Robo* was based on the same type of works in the commissural axon guidance defected *Drosophila* embryos (Seeger M. et al., 1993). Too many axons have crossed the midline in the *Robo* mutant embryos (Kidd T et al. 1998a ; Seeger M. et al., 1993) Product of *Robo* gene is a cell surface protein that is expressed on the central nervous system axons (Kidd T. et al., 1998a). In *Drosophila* there are three *robo* genes (*robo1 robo2 robo3*) and in mammals there are four: *Robo1 Robo2 Robo3 (*also known as Rig-1*)* and *Robo4* (Known as magic roundabout). All the vertebrate *Robo* genes, except *Robo*4, seem to be expressed in central nervous system.

Robo proteins have an extracellular domain comprising five immunoglobulin like and three fibronectin-III repeats with a single transmembrane segment and a cytoplasmic domain, which has no obvious catalytic activity (Kidd T. et al., 1998a). Exception to the general structure of Robo family is the magic roundabout that consists of two Ig domains and two FN3 domains. Slit binding site on the Robo proteins has been identified in the first two Ig domains (Liu Z. et al., 2004) that correspond to most conserved region in the Robo receptors (**Figure 1.3**).

The cytoplasmic domains of Robo receptors are not well conserved but they share four short conserved motifs. These motifs are named as CC0-3 and are thought to be sites of

interaction for various cytoplasmic signaling proteins. Ena/VASP proteins are one of these proteins and they bind to CC1 and CC2. Also SRC Homology Domain 2 and 3 (SH2 and SH3), adaptor Dock/Nck proteins bind to CC2 and CC3 motifs (Fan X et al. 2003). Rho family GTPase activating proteins Vilse/crGAP and srGAPS also bind to CC2 and CC3, respectively (Hu H. et al., 2005; Lundstorm A. et al., 2004; Wong K. et al., 2001). It is not clear how these signals interact with each other and repel the growth cone. Not all Robos have four CC domains. This in turn indicates that different Robos have different sets of cytoplasmic partners (**Figure 1.3-e**) and these different partners lead them to give different responses.

Three mammalian Robos (Robo1 Robo2 and Robo3) show a complex expression pattern in the neuronal populations. For example Robo1 and Robo2 levels are very low as the axons cross the midline and increase in crossed axons (Long H. et al.,2004). However Robo3 shows the opposite pattern which is high before crossing and low afterwards (Sabatier C. et al., 2004). This expression pattern brought about the following question: What is the mechanism that keeps Robo1 and Robo2 levels low in commissural axons during the midline crossing? The answer was found in the *comm.* (commissureless) gene (Tear G et al., 1996) that has been revealed in the same mutants that had allowed the identification of *robo* gene. In the *comm* mutants no axons cross the midline. This data suggested that normal function of Comm is to antagonize the Slit-Robo function and allow the midline crossing. Comm does this job by functioning as an endosomal sorting receptor for Robo (Keleman K. et al., 2002). Comm is localized in the Golgi and in late endosomes (**Figure 1.4**).

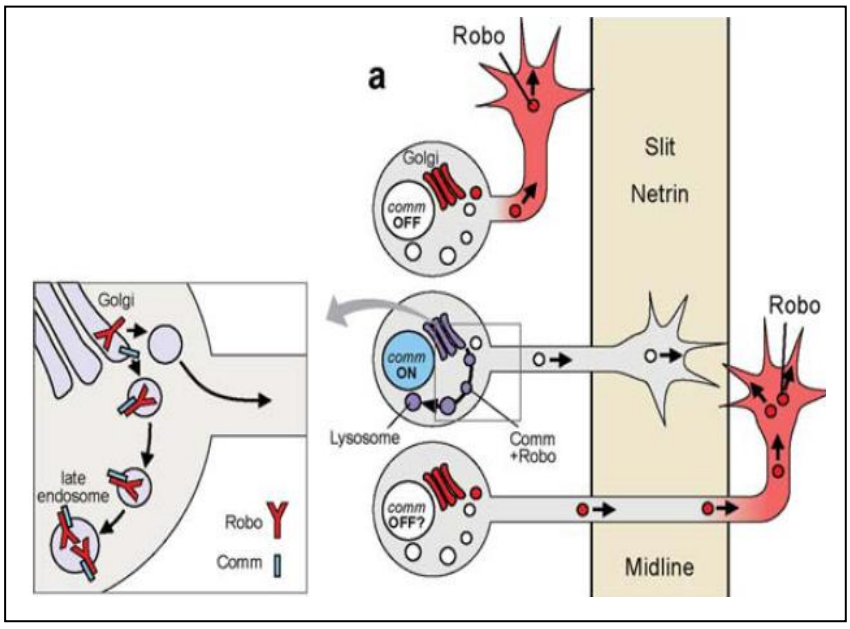

Figure 1.4: A model for sorting of Robo by *Comm.* (Dickson and Gilestro et al., 2004)

It can bind to Robo and recruit it to the endosomes. Without Comm Robo is normally transported down the axons but this transportation is blocked by Comm. In vertebrates, no homologues of Comm could be found. Instead of a vertebrate Comm, researchers found a surprising negative regulator of Slit-Robo signaling. This negative regulator is Robo3 (Rig-1) protein which was expected to function positively on the Slit signaling like other Robo's, but it did not. *Robo3-/-* embryos' commissural axons mimic the *comm* mutant phenotype and all of the commissural axons avoid the midline (Sabatier C. et al., 2004). Expression pattern of Robo3 revealed its expected role. Its expression is strictly restricted along the commissural axons but in an opposite manner of Robo1 and Robo2. Robo3 levels are high before crossing and low after crossing (Sabatier C. et al., 2004) (**Figure 1.5)**. It is obvious that Robo3 allows crossing of the commissural axons by inhibiting Slit- Robo1 signaling.

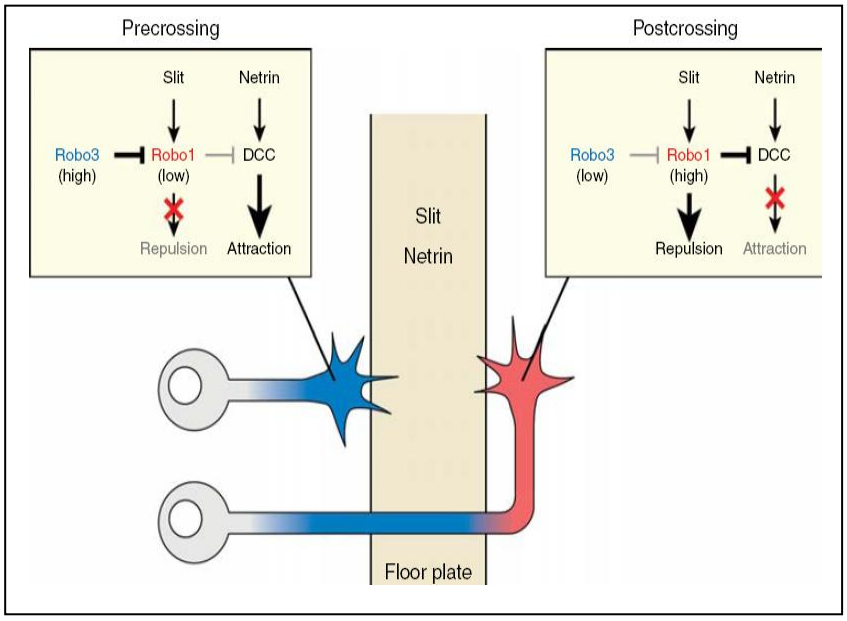

Figure 1.5: Robo3 antagonizes Robo1 to allow crossing in mice. Model adapted from Sabatier et al. (2004). In pre-crossing commissural axons, Robo3 levels are high, and Robo1 levels low. Robo3A is thought to inhibit Robo1-mediated repulsion in these axons (Sabatier et al. 2004) so that they are instead attracted to the floor plate by netrin-1 and sonic hedgehog. After crossing, Robo3 levels are low, and Robo1 levels high. Axons are now repelled by signaling of Slit through Robo1.In addition, attraction to netrin-1 may be downregulated, possibly owing to a Slit-dependent interaction between Robo1 and the netrin receptor DCC. (Dickson and Gilestro et al., 2004)

1.3.2 ROBOs and SLITs Role in Other Developmental Steps:

1.3.2.1 Kidney Bud Development:

Kidney development occurs along the body axis and it begins with the emerging of a single uteric bud from the nephric duct (Saxen L. et al., 1987). This emergence is a response to GNDF secretion from the adjacent nephrogenic mesenchyme (Moore M.W. et al., 1996). Important point in the correct positioning of the uteric bud is the restriction of GNDF expression to the posterior (Pachnis V. et al 1993). Anterior expansion of GNDF expression is correlated with supernumerary uteric bud formation (Kume T. et al., 2000). Grieshammer and colleagues have shown that inactivation of either *Slit2* or *Robo2* in mice leads to supernumerary bud development and that this is correlated with abnormal maintenance of *Gndf* expression in anterior nephrogenic mesenchyme (Grieshammer U. et al., 2004). *Gndf* dosage reduction in *Slit2 -/-* animals results in the rescue of this phenotype. **(Figure 1.6)**

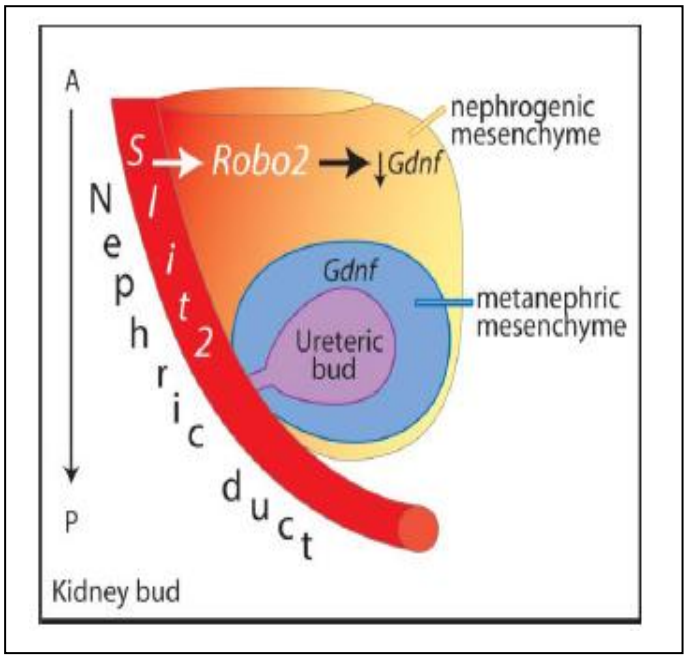

Figure 1.6: Uteric bud formation. GNDF expression is restricted to posterior by the act of SLIT2 triggered ROBO2. Inactivation of either the SLIT2 or ROBO2 leads to supernumerary bud formation because of the increased levels of GNDF expression in anterior. (Grieshammer et al., 2004)

1.3.2.2 Endothelial Cell Migration and Angiogenesis:

Robo4 is the most recently discovered member of the Roundabout family. It was identified in a data mining for endothelial specific genes (Huminiecki L.et al., 2000; 2002). Genes that belong to ROBO-SLIT family and expressed in the endothelial cells is not restricted to only ROBO4. Wu et al showed that Slit2 and Slit3 mRNAs but not Slit1 were expressed in the rat endothelial cells (Wu JY. et al., 2001). In 2008 Jones AC. and colleagues recognized the similarities between the angiogenic sprout and growing axon and found that Robo4 maintains the vascular integrity by inhibiting the pathologic angiogenesis and endothelial hyperpermeability. Inhibition of pathologic angiogenesis is through the inhibition

of VEGF-165 by Robo4/Slit2 axis. This inhibition also decreases the permeability levels of the vascular network (Jones C.A. et al., 2008).

1.3.2 ROBO-SLIT Family and Cancer

Deletion and epigenetic inactivation of Slit-Robo genes have been identified in different cancers. Inactivation of Robo1 results in frequent mortality. Those that survive have developed bronchial hyperplasia (Xian J. et al., 2001). This result showed that Robo1 is a tumor suppressor gene. Real time PCR analysis of seven normal prostate and 48 prostate tumors has shown that Robo1 expression is downregulated in the prostate cancer (Latil A. et al., 2003). The *DUTT1/ROBO1* gene was isolated from the U2020 region (Sundaresan V. et al., 1998a) and this region overlaps with the common deletion site in (NCI-H2196) SCLC cell lines. This deletion abrogates exon 2 of the gene.

Dallol A. and colleagues analyzed the *DUTT1* gene expression in lung, breast and kidney tumor lines and the presence of mutations in lung, breast, kidney tumors and tumor cell lines. They didn't find any inactivating mutations but loss of expression in breast tumor cell lines was due to the promoter hypermethylation. 5-aza-2'-deoxycytidine (5-Aza-dC) treatment rescued the expression of *DUTT1* gene in this cell line. It was shown that SLIT2 is also epigenetically inactivated in 40% of lung and breast tumors, 72% of the primary colorectal cancers and 71% of the glioma cell lines. Expression is restored by 5-Aza-dC treatment (Dallol A. et al., 2003a; 2003b).

Dickinson RE and colleagues checked the expression profile of Slit 1, which is mainly expressed in neural tissues, and Slit3 gene, which has more widely expression pattern than Slit1, both in cancerous and normal tissues. After this analysis Slit3 was found to be methylated in 41% of breast, 33% of colorectal and 29% of glioma tumor cell lines whereas Slit1 was found to be methylated in 83% of glioma tumors (Dickinson RE., et al., 2004).

SLIT1, SLIT2 and SLIT3 expression in hepatocellular carcinoma was found to be very low in poorly differentiated cell lines (Ito H., et al., 2006). This finding may set a connection between the tumor progression and Slit Family.

In 2003 Wang showed that Robo1-Slit2 signaling pathway is activated in the angiogenically active sites of the tumor. Recombinant Slit2 protein attracted the endothelial cells and promoted the tube formation in a Robo1 and PI kinase dependent manner. Neutralization of Robo1 dramatically reduced the microvessel density and also the tumor mass of the malignant melanoma A375 cells *in vivo* (Wang B. et al., 2003).

Slit2 treatment of the breast cancer cells was shown to inhibit the CXCL12/CXCR4 induced breast cancer cell chemotaxis, chemoinvasion and further adhesion of the cells to the new environment, which are the fundamental components of the tumor metastasis (Prasad A. et al.,2004). In 2008, the same group proved that Slit2 induces a tumor suppressive effect by coordinated regulation of B catenin and PI3K signaling pathways and by enhancing the β catenin/E cadherin mediated cell-cell adhesion. Also Slit2 over expressing MCF-7 cells showed 60-70% reduction in the tumor size compared with the mice injected with normal MCF-7 cells (Prasad A. et al., 2008).

In a recent work it was proved that SLIT2 expression is downregulated in 75% of HCC cell lines and 83.3% of HCC samples. Decrease in the expression is significantly correlated with the CpG island hypermethylation. Furthermore, expression of SLIT2 was restored after treatment of 5-Aza-dC treatment (Jin J. et al., 2009).

In 2006, Ito H. and colleagues find out that ROBO1 is overexpressed in 83 of 98 cases of HCC (84.7%). Also they detected the ectodomain of ROBO1 in both the medium of liver cancer cell lines (PLC and HepG2) and sera from HCC patients. (Ito H. et al., 2006)

2. AIM OF THE STUDY

Analysis of differentially expressed genes between tumor and normal tissue is one of the gold standards for a better understanding of carcinogenesis. Genes identified in such studies not only strengthen cancer research works, but also provide valuable tools for early diagnosis, effective monitoring of disease progression and reveal new therapeutic targets.

Hepatocellular carcinoma (HCC) is one of the most wide-spread carcinomas throughout the world –responsible for 600,000 deaths annually. Diagnostic, prognostic tools and effective therapies for this aggressive cancer are very limited. Therefore the understanding of molecular pathways underlying HCC is of great importance.

Recently, our group showed that transcripts of SLIT-ROBO family of genes (SLIT1-3, ROBO1-4) are differentially expressed in HCC. In the last few years, it was also shown that ROBO1 is overexpressed and SLIT2 is epigenetically inactivated in liver cancer. On the other hand, ROBO4 expression was found to be generally confined to vascular endothelium. Therefore, to complete the understanding of the regulation of expression of ROBO SLIT family genes in HCC, we decided to study whether SLIT1, SLIT3, ROBO2, and ROBO3 are epigenetically regulated by means of hypermethylation of their gene regulatory regions.

CHAPTER 3 MATERIALS AND METHODS

3.1 MATERIALS

3.1.1 Reagents

All laboratory chemicals were analytical grade from Sigma-Aldrich (St.Louis, MO, USA), Farmitalia Carlo Erba (Milano, Italy) and Merck (Schucdarf, Germany) with the following exceptions: ethanol and methanol were from Riedel-de Haën (Germany). Agar, tryptone and yeast extract were obtained from Gibco (Carlsbad, CA, USA), BRL Life Technology Inc. (Gaithersburgs, MD, USA).

3.1.2 Bacterial Strains

The bacterial strain used in this work was *E.coli* DH5α.

3.1.3 Enzymes

Restriction endonucleases used for gene cloning were purchased from Jena Bioscience (Germany). T4 DNA ligase was purchased from Fermentas GmbH (Germany). DyNAzyme II and Phusion DNA Polymerase was purchased from Finnzymes (Espoo, Finland).

3.1.4 DNA Markers

DNA molecular weight standards were purchased from Fermentas GmbH (Germany) (100 bp-SM0241, 1kb-SM0311) and Jena Bioscience (Germany) (low range DNA ladder 50-1000 bp, high range DNA ladder 0.5-10kb).

3.1.5 Oligonucleotides

The oligonucleotides used in polymerase chain reactions were synthesized and supplied from Iontek Inc. (Istanbul, Turkey) and Alpha DNA (Germany).

3.1.6 Plasmids

pGL3 Luciferase Reporter Vector was purchased from PROMEGA Corporation (USA). e1b TATA box added modified version of pGL3 was kindly provided by Hani Alotaibi.

3.1.7 Electrophoresis, photography and spectrophotometer

Electrophoresis grade agarose was obtained from Sigma Biosciences Chemical Company Ltd. (St. Louis, MO, USA). Horizontal electrophoresis apparatuses were from E-C Apparatus Corporation (Florida, USA). The power supply Power-PAC300 and Power-PAC200 was from Bio Rad Laboratories (CA, USA). The Molecular Analyst software used in agarose gel profile

visualizing was from Vilber Lourmat (France). Beckman Spectrophotometer Du640 was purchased from Beckman Instruments Inc. (CA. USA) and Nanodrop ND-1000 Full-spectrum UV/Vis Spectrophotometer was purchased from Thermo Fisher Scientific (Wilmington, DE, USA). The Reporter Microplate Luminometer Reader was from Turner BioSystems Inc (Sunnyvale, CA, USA).

3.1.8 Tissue culture reagents and cell lines

Dulbecco's modified Eagle's medium (DMEM), RPMI 1640, trypsin, non-essential amino acids, penicillin/streptomycin mixture and fetal calf serum were obtained from HyClone (South Logan, UT, USA). Tissue culture flasks, petri dishes and cryotubes were purchased from Costar Corp. (Cambridge, England). Geneticin-G418 sulfate was purchased from GibcoBRL (Carlsbad, CA, USA).

3.1.9 Transfection reagents

FuGene HD (Roche, Mannheim, Germany) and Licofectamine 2000 (Invitrogen, Carlsbad, CA, USA) transfection reagents were used in this study. OptiMEM I serum free medium was purchased from Invitrogen (Carlsbad, CA, USA).

3.1.10 Kits

RNeasy Mini Kit was obtained from Qiagen (Hilden, Germany). NucleoSpin RNA II Kit was obtained from Macherey-Nagel (Duren, Germany). DyNAmo cDNA Synthesis Kit and DyNAmo™ HS SYBR® Green qPCR Kit were purchased from Finnzymes (Espoo, Finland). Qiaprep spin mini-prep kit (for small scale DNA isolation), Qiafilter plasmid midi kit (for medium-scale DNA isolation), Qiaquick PCR purification and gel extraction kits (for recovery and extraction of DNA from agarose gel) were from Qiagen (Hilden, Germany). UltraClean Tissue DNA Isolation Kit was purchased from MOBIO Laboratories (Carlsbad, CA, USA). Bisulfite treatment kit was obtained from EPIGENTEK MethylAMP® DNA modification kit (NY, USA)

3.2 SOLUTIONS AND MEDIA

3.2.1 General solutions

Tris-acetic acid-EDTA (TAE): Stock solution (50XTAE) was prepared by addition of 121g Tris-base, 18.6g EDTA, and 28.55ml glacial acetic acid to 500ml ddH_2O. pH of the stock solution was adjusted to 8.5. Working solution (1XTAE) was prepared by dilution of 50XTAE to 1X with ddH_2O.

Ethidium bromide: 10mg/ml in water (stock solution), 30ng/ml (working solution).

6X Agarose gel loading dye: A mixture of 0.009g bromophenol blue (BFB), 0.009g xylene cyanol (XC), 2.8ml ddH2O, 1.2ml 0.5M EDTA was prepared. The total volume was brought to 15ml by addition of glycerol.

3.2.2 RNA solutions

DEPC-treated water: 1ml DEPC was added to 1L ddH_2O and stirred under hood overnight. DEPC was inactivated by autoclaving.

3.2.3 Microbiological media, reagents and antibiotics

Luria Bertani (LB) medium: Per liter; 10g bacto-tryptone, 5g bacto-yeast extract, 10g NaCl. For LB agar plates, 15g/L bacto agar was added.

Glycerol stock solution: A final concentration of 25% glycerol in LB was added to bacterial culture.

Ampicillin: 100mg/ml solution in ddH_2O, sterilized by filtration and stored at -20°C (stock solution). Working solution was 100µg/ml.

SOB medium: Per liter; 20g tryptone (2%), 5g yeast extract (0.5%), 0.584g NaCl (10mM), 0.1864g KCl (2.5mM) autoclaved to sterilize. Then, 2.46g MgSO4 and 2.03g MgCl2 (10mM) are added.

SOC medium: SOB + 20mM glucose from filter sterilized 1M glucose stock solution in ddH2O.

Transformation buffer (TB): 10mM PIPES, 55mM $MnCl_2$, 15mM $CaCl_2$, 250mM KCl. Filter sterilized and stored at 4^oC.

3.2.4 Tissue culture solutions

DMEM/RPMI1640 growth media: 10% FBS, 1% penicillin/streptomycin, 1% non-essential amino acid were added and stored at 4^oC.

Freezing solution: 10% DMSO and 90% FCS were mixed freshly.

Phosphate buffered saline (PBS): Stock solution (10XPBS) was prepared by dissolving 80g NaCl, 2g KCl, 17.8g $Na_2HPO_4.2H_2O$, and 2.4g KH_2PO_4 in 1L ddH2O. Working solution

(1XPBS) was prepared by dilution of 10XPBS to 1X with ddH_2O. pH of the working solution was adjusted to 7.4.

3.3 METHODS

3.3.1 General methods

3.3.1.1 Bacterial transformation

3.3.1.1.1 Super-competent E.coli preparation

Super-competent *E.coli* preparation was described by Inoue (Inoue H. et al., 1990). *E.coli* DH5α cells were grown in SOB medium at 30^{o}C to an $O.D._{600}$ of 0.5-0.6 with vigorous shaking at 225rpm and cooled down on ice for 10 minutes. Cells were transferred to 500ml centrifuge bottles and centrifuged at 2500g for 10 minutes (Beckman JA10 rotor, pre-cooled to 4^{o}C). The pellet was resuspended in ice-cold transformation buffer (1/3 of initial culture volume) by gently swirling and kept on ice for 10 minutes. The suspension was then centrifuged at 2500g for 10 minutes. The pellet was gently re-suspended in ice-cold transformation buffer (1/12.5 of initial culture volume) then DMSO was added with gently swirling to a final concentration of 7% and incubated on ice for 10 minutes. Super-competent cells were aliquotted to 1.5ml eppendorf tubes, then immersed in liquid nitrogen to snap-freeze and stored at -80^{o}C.

3.3.1.1.2 Super-competent E.coli transformation

Super-competent cells were thawed on ice for ~15minutes. From this, 150µl of cells were pipetted to pre-chilled transformation tubes and immediately mixed with the ligation products or 10ng intact plasmid. Then the complex was incubated on ice for 30 minutes, after which a heat-shock at 42^{o}C for 30-45 seconds applied. Heat-shocked cells were immediately replaced on ice for 2 minutes and consequently 850µl LB medium was added. For antibiotic resistance gene to be expressed, the cells were rotated at 225rpm for 1hour in a 37^{o}C shaker. If ligation product was used then the cells were pelleted and re-suspended in 100µl LB; otherwise when intact plasmid was used, 100µl from 1ml total culture was taken and spread on agar plates with suitable selection antibiotic. Under aseptic conditions, plates were left to drain for ~10minutes and then placed in an inverted position into 37^{o}C incubators for overnight (12-16 hours). Next day the emerging colonies were collected for mini-prep.

3.3.1.2 Long term storage of bacterial strains

To keep bacterial cells including plasmid in it or as empty for future experiments and to have a stock of strain in a laboratory is necessary. The most frequently used method is "Glycerol-Stock" method. A single colony picked from either an agar plate or a loop-full of bacterial stock was inoculated into 5ml LB (with a selective agent if necessary) in 15ml screw capped tubes. Tubes were incubated overnight at 37^{o}C and at 225rpm. For glycerol stock, 500µl of saturated culture was added into 700ul of 50% glycerol v/v. This mix was frozen/stored at -80^{o}C.

3.3.1.3 Plasmid DNA preparation

Small scale isolation of plasmid DNA was performed with Qiaquick spin mini-prep kit according to the manufacturer's instructions. This procedure yields approximately 200ng/µl of plasmid DNA for 1ml of LB culture. For large-scale preparation of pure plasmid DNA, the Qiafilter plasmid midi kit was used by following the manufacturer's instructions. This procedure yields approximately 1µg/µl of plasmid DNA for 100 ml of LB culture.

3.3.1.4 Preparation of genomic DNA from cultured cells

Cultured cells were grown in 100mm tissue culture dishes to 70-80% confluency, trypsinized, and washed with 1XPBS. Genomic DNA was isolated by using UltraClean Tissue DNA Isolation Kit (MOBIO Laboratories, Carlsbad, CA, USA) following manufacturer's instructions.

3.3.1.5 Extraction of total RNA from tissue culture cells

Exponentially growing monolayer cultures were washed twice with ice-cold PBS, scraped with a scraper, pelleted at +4^{o}C and stored at -80^{o}C until needed for RNA preparation. The total RNA isolation from cell line pellets was performed directly by use of NucleoSpin RNA II kit according to the manufacturer's instructions. The RNAs were eluted in a total volume of 40µl. The concentration of the isolated RNA and O.D.260/280 ratio were measured with the NanoDrop ND-1000 spectrophotometer (NanoDrop Technologies, Montchanin, DE, USA). Isolated RNAs were snap-frozen with liquid nitrogen and stored at -80^{o}C.

3.3.1.6 Quantification and qualification of nucleic acids and proteins

Concentration and purity of the double stranded nucleic acids (plasmid and genomic DNAs) and total RNAs were determined by using the RNA and double-stranded(ds) DNA methods on Nanodrop ND-1000 Full-spectrum UV/Vis Spectrophotometer (Thermo Fisher Scientific, Wilmington, DE, USA). Concentration and purity of proteins were determined by using the

Beckman Instruments Du Series 600 Spectrophotometer software programs on the Beckman Spectrophotometer Du640 (Beckman Instruments Inc. CA. USA).

3.3.1.7 Restriction enzyme digestion of DNA

Restriction enzyme digestions were routinely performed in 20µl or 50µl reaction volumes and typically 5-10µg DNA was used. Reactions were carried out with the appropriate reaction buffer and conditions according to the manufacturer's recommendations. Digestion of DNA with two different restriction enzymes was also performed in the appropriate common reaction buffer and conditions recommended by the manufacturer.

3.3.1.8 Agarose gel electrophoresis of DNA

DNA fragments were fractionated by horizontal gel electrophoresis in 1-2% (w/v) agarose gel by using 1XTAE buffer. DNA fragments less than 1 kb were generally separated on 1.0% or 2.0 % agarose gel, those greater than 1 kb (up to 11 kb) were separated on 1 % agarose gels. Agarose was completely dissolved in 1XTAE electrophoresis buffer in the desired percentages and ethidium bromide solution was added to final concentration of 30ng/ml. 6XDNA loading dye was added to 10µl of quantitative real time RT-PCR (QRT-PCR) products and 20µl of normal PCR products such that the final dye concentration will be 1X, and total volume was loaded to each well. Nucleic acids were visualized under ultraviolet light (long wave, 340nm) and GeneRuler (Fermentas) DNA size markers was used to estimate the fragment sizes.1 kb DNA ladder was loaded for products sizes of over 1kb and 100 bp ladder for product sizes of below 1kb.

3.3.2 Tissue culture techniques

3.3.2.1 Cell lines

13 hepatoma (Huh7, FOCUS, Mahlavu, Hep40, Hep3B, PLC/PRF/5, SK-Hep1, Snu182, Snu387, Snu398, Snu423, Snu449 and Snu475) and 1 hepatoblastoma (HepG2) cell lines were used in this study and cultured as previously described (Cagatay T. and Ozturk M., 2002)

3.3.2.2 Thawing cryopreserved cells

One vial of the frozen cells from the liquid nitrogen tank was taken and immediately put into ice. The vial was left 1 minute on the bench to allow excess nitrogen to evaporate and then placed into 37^{o}C water bath until the external part of the cell solution was thawed (takes approximately 1-2 minutes). The cells were directly poured into a 15ml sterile tube containing

10ml cold fresh medium. The cells were centrifuged at 1500rpm at 4^{o}C for 5 minutes. Supernatant was discarded and the pellet was resuspended in 10ml 37^{o}C culture medium to be plated into 100mm dish. After overnight incubation in a humidified incubator at 37°C supplied with 5% CO2, culture mediums were refreshed.

3.3.2.3 Growth conditions of cell lines

Focus, Hep40, Hep3B, Hep3B-TR, HepG2, HUH7, Mahlavu, PLC/PRF/5, SK Hep1 cells were cultured in low-glucose DMEM supplemented with 10% FBS, 100U/ml Penicillin-Streptomycin, and 0.1mM non-essential amino acids (HyClone, Utah, USA). SNU387, SNU398, SNU423, SNU449, SNU475 cells were cultured in RPMI1640 medium supplemented with 10% FBS, 100 U/ml Penicillin-Streptomycin, 0.1mM non-essential amino acids (HyClone, Utah, USA). The growth medium was aspirated and the cells were washed once with 1XPBS. Trypsin was added to the flask to remove the monolayer cells from the surface. The fresh medium was added and the suspension was pipetted gently to disperse the cells. The cells were transferred to either fresh petri dishes or fresh flasks using different dilutions (from 1:2 to 1:10) depending on requirements. All media and solutions used for culture were kept at 4°C (except stock solutions) and warmed to 37°C before use.

3.3.2.4 Cryopreservation of cell lines

Exponentially growing cells were harvested by trypsinization and neutralized with growth medium. The cells were counted and precipitated at 1500rpm for 5min. The pellet was suspended in a freezing solution (10%DMSO, 20%FCS and 70%DMEM for adherent cells) at a concentration of ~4x10^{6}cells/ml. 1ml of this solution was placed into 1ml screw capped cryotubes. The tubes were first frozen at -20^{o}C for 0.5-1hours and then left at -80°C overnight. The next day, the tubes were transferred into the liquid nitrogen storage tank.

3.3.2.5 Transient Transfection of Cell Lines:

3.3.2.5.1 Transient Transfection of Eukaryotic Cells Using with “Lipofectamine Reagent”

Transfection was performed with Lipofectamin 2000 reagent (Invitrogen) following manufacturer’s instructions.

3.3.2.5.2 Transient Transfection of Eukaryotic Cells Using with FuGene HD:

Transfection was performed with FuGene HD reagent (Invitrogen) following manufacturer’s instructions.

3.3.2.6 5-Aza-dC Treatment of the Cells

5-Aza-dC stock solutions was prepared with the concentration of 100uM in DMEM. Cells were treated with 2.5 uM of 5-Aza-dC for 4 days.

3.3.3 cDNA synthesis

cDNA was synthesized by using DyNAmo^{TM} cDNA Synthesis Kit (Finnzymes, Espoo, Finland) according to manufacturer's instructions. Briefly; for 1X reaction 1µg of total RNA, 1µl oligo(dT) primers or 1 µl random hexamers and required amount of ddH_2O were mixed in a total 8µl volume, then incubated at 65°C for 5min and chilled on ice. Then, 4 µl of 5X First Strand Buffer, 1 µl of RNase inhibitor and 2 µl of deoxynucleotide triphosphate mix (10 mM) were added and the reaction was incubated at 37°C for 5 min. Finally, the mixture was incubated at 42oC for 1 hr with 1 µl of reverse transciptase enzyme. The reaction was stopped by heating the mixture for 10 min at 70oC. Each cDNA sample was diluted at a ratio of 1:5 with ddH2O and stored at -20oC to be used as a PCR template for further experiments. The oligo(dT) primed cDNA samples were used for the analysis of all the target and reference genes included in this study.

3.3.4 Primer design for Cloning and MS-PCR

The primer pairs that have been used in cloning were as follows: Forward primers F1, F2, F3, F4 for putative promoter region were selected from the beginning part of the CpG island, beginning of the promoter, end of the promoter and end of the CpG island respectively. Primers used for amplifying the *ROBO2* CpG island by MS-PCR was designed by MethPrimer website. Other MS-PCR primers were previously described (Nguyen et al., 2006). All Primers were listed in Table 3.1.

TABLE 3.1 LIST OF PRIMERS

#	Primer Name:	Sequence:
1	F1 e1b	TGCACACGCGTCCTTCCTCCTACTCGGCTTC
2	F2 e1b	TGCACACGCGTGCAGACGGAGGGATGAATAA
3	F3 e1b	TGCACACGCGTCGCCTTCCCTCCTAGAAGTC
4	F4 e1b	TGCACACGCGTCTTTTGGAAACCGGAGAGGT

5	Reverse (-F4) e1b	TGCACCTCGAGCTCCTTTGCAGCGGTGTT
6	Reverse (full length) e1b	TGCACCTCGAGTTTGACATATTAAAAAGGATCCAG
7	Enhancer Wide Forward	CCATTGGAGAAAACCTCAAAA
8	Enhancer Wide Reverse	GGTGGCATTGTAGCTGTCCT
9	Enhancer true F	TGCACGGATCCCATGGGAATATTGAGTCCTTATCA
10	Enhancer true R	TGCACGTCGACCCTTCCTCTTGGCAAGTCTG
11	R2 PRO-R	GCAGACCCATGGTGACATATTAAAAAGGATCCAG
12	R2 PRO-F1	TGCAC AAGCTT CCTTCCTCCTACTCGGCTTC
13	R2 PRO-F2	CGCAC AAGCTT GCAGACGGAGGGATGAATAA
14	R2 PRO-F3	TGCAC AAGCTT CGCCTTCCCTCCTAGAAGTC
15	R2 PRO-F4	TGCAC AAGCTT CTTTTGGAAACCGGAGAGGT
16	R2 PRO-R5	GTCCACCATGGCTCCTTTGCAGCGGTGTT
17	R2PW-F	CCACACCCAGAGCCT
18	R2PW-R	AGGCTCTTGCAGGAGATTGA
19	SLIT1-UR2	ttttcctcctcAcaAcaAtcaA
20	SLIT1-UF2	TgggTttgTgTgTggTgTTT
21	SLIT1-MR2	aAAcgccgtcgcttAAaAA
22	SLIT1-MF2	TtcgTtcgcgagTTagacg
23	SLIT3-MF	ggtttcgtcgatggagttgt
24	SLIT3-MR	aaacgcgtaaaacccgaaa
25	SLIT3-UF	TGTGggTTagTGgggTTagg
26	SLIT3-UR	cacaaacaaaacaaaacactcca

27	ROBO1-MF2	cggcggcgatagTagTTaaa
28	ROBO1-MR2	cgAAActAAAAAcgcccaAa
29	ROBO1-MF3	cggcgtgcgTTTTTaTaatg
30	ROBO1-MR3	gccAcgAAtAAcccgctAct
31	ROBO1-UF	TggTggTaaagttggggtgt
32	ROBO1-UR	ccAaAcccttcctccAAaAc
33	ROBO3-MF	gcgggaTtTtTagTcggTTT
34	ROBO3-MR	gAcctctccgcaAActAAcg
35	ROBO3-UF	TggTgggaTtTtTagTTggTTT
36	ROBO3-UR	ccAcaActtccccAcAAcAc
37	ROBO2-MF	TATTATTTTTAGAGGCGGTATCGC
38	ROBO2-MR	AATAAAAAATCCGAACTCCTACGTA
39	ROBO2-UF	ATTATTTTTAGAGGTGGTATTGTGG
40	ROBO2-UR	AATAAAAAATCCAAACTCCTACATA
41	SLIT1 F	GACGTGGTCTGTCCCCACAA
42	SLIT1 R	AATCTCATTGTTATTCAATCGCAGTT
43	SLIT3 F	CCGCCTAACTACACAGGTGAGCTAT
44	SLIT3 R	CGCTGTAGCCAGGGACACACT
45	ROBO2 F	GGGTTACTACATCTGCCAGGCTT
46	ROBO2 R	AGGTGGAGGTCTATCTGTCAAAACAT
47	ROBO3 F	CAGTGTCCGATGGAAGAAGG
48	ROBO3 R	GTCCATCTCCTGCACATTGG

49	GAPDH F	GGCTGAGAACGGGAAGCTTGTCAT
50	GAPDH R	CAGCCTTCTCCATGGTGGTGAAGA
51	GL2	GGAAGACGCCAAAAACATAAAG
52	RV3	CTAGCAAAATAGGCTGTCCC
53	RV4	CGCGGGGCATGACTATCGTC

TABLE 3.2 PRIMER EFFICIENCIES & PRODUCT SIZES FOR REAL TIME PCR PRIMERS:

PRIMER	EFFICIENCY	PRODUCT SIZE
Robo2	1.9	98
Robo3	1.9	106
Slit1	1.9	130
Slit3	2.0	136
Gapdh	2.0	143

3.3.5 Fidelity and DNA contamination control in first strand cDNAs

The fidelity and genomic DNA contamination of first strand cDNAs were checked before performing expression analyses. 2µl of diluted first strand cDNA was used for cold-PCR amplification of the glyceraldehyde-3-phosphate dehydrogenase (GAPDH) transcript. GAPDH primer pair for this analysis was designed to produce a 151 bp fragment from cDNA and 250 bp fragment from genomic DNA.

3.3.6 Methylation Specific PCR

Bisulfite treated DNA of HCC cell lines were eluted in 8µl of elution buffer. PCR volume is 50 µl. Briefly, reaction content is: 1µl of DynAzyme II, 5 µl of dNTP (2mM), 4 µl of bisulfite treated DNA, 1.5 µl of Mg^{2+}, 5 µl of PCR Buffer (10X) and 33.5 ul of ddH_2O. Reaction conditions are as follows: 95^{o}C 15 min, (94^{o}C 30 sec, 58^{o}C 30 sec, 72^{o}C 40 sec) 45 cycles, and final extension at 72^{o}C for 10 min.

3.3.7 Cloning Strategies for ROBO2 Putative Promoter and Enhancer:

During the cloning works Phusion® DNA Polymerase FINNZYMES were used because of its high proof reading activity, low mutation rate and increased specificity. To synthesize the fragments of putative promoter region, nested PCR primers (R2PW-F& R2PW-R) were used and extended fragments were obtained. Then, these fragments were used as DNA source of the next PCR. Reverse primer (R2-PRO-R) contains 3 mispriming bases which are not

complementary to the genomic DNA. Mispriming bases at the 3' end of the R2-PRO-R gene was designed to fit into translation start site of *luc* gene, *NcoI* restriction site, the end of the 5' UTR of *ROBO2* gene just before the translation start site. These first constructs contain *NcoI* and *HindIII* restriction sites. Putative enhancer region was also amplified from the nested PCR product. Then enhancer region insert with *SalI and BamHI* restriction sites. Inserts for e1b pGL3 vector contains *MluI and XhoI* restriction sites and synthesized from the nested PCR product made with R2PW-F& R2PW-R. Exclusion of F4 region from these constructs were made by using the same forward primes of F1,2,3,4 synthesis both for pGL3 basic and e1b but the reverse primers were different. "Reverse (-F4) e1b" & "R2 PRO-R5" primers were used. PCR reactions were performed in 50 µl: 10 µl of Phusion GC- Buffer, 0.6 µl of Phusion DNA Polymerase, 5 µl dNTP, 2 µl of genomic DNA (or nested PCR product), and 32.4 µl ddH_2O with 98^oC 3 min, (98^oC for 10 sec, 60^oC for 15 sec, 72^oC for 45 sec)45 cycles, 72^oC for 10 min for final extension. All inserts cut and isolated from the gel. Then, they exposed to restriction enzymes for 4 hours. 1µg of DNA were cut for each insert in 50µl volume which contains 5 µl of restriction enzyme buffer, 1 µl of enzymes. Restriction products were purified with Qiagen PCR Purification Kit. Ligations of the inserts to vectors were performed with T4 DNA ligase in 10 µl volume which contains 100 µg vector and required amount of DNA, 1 µl of ligation buffer, 1 µl of T4 DNA ligase and ddH_2O. Required insert amount was calculated with the following formula: ng of insert = [(ng of vector X kb size of insert) / kb size of vector] X molar ratio of insert/ vector (which is 1/3).

3.4 Quantitative real time RT-PCR

Real-time qRT-PCR was performed on BioRad iCycler (Bio-Rad, California, USA) using the BioRad iQTM SYBR Green Supermix. The amplification mixtures contained 1.0 µl of 1:5-diluted cDNA template, 6.25 µl SYBR Green PCR Master Mix Buffer (2X), and 10 pmol of forward and reverse primers in a total volume of 12.5 µl. The cycling conditions were as follows: an initial incubation of 95°C for 5 min and then 45 cycles of 95°C for 30 s and 60°C for 30 s during which the fluorescence data were collected. To verify that the used primer pair produced only a single product, a dissociation protocol was added after thermocycling, determining dissociation of the PCR products from 55°C to 95°C in 80 cycles. 12.5µl mineral oil was added to cover top of the mixture to prevent evaporation. The amplification reactions were performed in 96 well-PCR plates and the plates were sealed with optical sealing tapes (Bio-Rad, California, USA). All PCR reactions were studied in duplicate. Treated and untreated samples were always analyzed in the same run to exclude between-run variations

and each sample was studied in duplicate. A no-template control of nuclease-free water was included in each run. Following amplification, a reaction product melt curve was obtained to provide evidence for a single reaction product. The iCycler iQ Optical System Software (version 3, BioRad Laboratories) was used to determine the melting temperatures of the products. The threshold cycle (Ct) value was calculated as the cycle where the fluorescence of the sample exceeded a threshold level.

In cell lines and tissues, the relative expression ratio (R) of *SLIT-ROBO* in 5-Aza dC treated and non treated cells were measured based on a modified ΔΔCt formula (35) and normalized to *GAPDH* or *ACTB* (reference gene). In $R= (E_{target})^{\Delta Ct_{target}^{(control-sample)}} / (E_{ref})^{\Delta Ct_{ref}^{(control-sample)}}$ formula E_{target} and E_{ref} reflect PCR efficiencies of the primers for target genes and reference genes, respectively. PCR efficiency values for each primer pair was obtained by constructing a standard curve using threshold cycle (Ct) values derived from 6 data points, corresponding to 2-fold decrements of an original cDNA stock (duplicates were prepared for each dilution). The slope of the resulting curve was used to calculate the E value of primer pairs according to $E = 2^{-1/slope}$ formula. PCR efficiencies of the genes ranged between 1.9 and 2.0. ΔCt was the difference between the Ct values of controls and samples.

3.5 Computer Analysis:

The sequences of the cloned FAM134B isoforms and of their mouse homologues were obtained from NCBI (National Center for Biotechnology Information) and UCSC (University of California, Santa Cruz) Genome Browser. The exon-intron information of these genes was derived using Ensembl Genome Browser at *http://www.ensembl.org*. Restriction endonuclease maps of the plasmid DNAs were analyzed by using the Clone.exe program. Primers were designed by using Primer.exe program provided by Whitehead Institute for Biomedical Research. The results of the DNA sequencing of engineered constructs were visualized using Finch TV 1.4 available for download at *http://www.geospiza.com/finchtv.html*. The alignments of nucleic acids was performed by using the NCBI Blast2Sequences algorithm available at the web page http://www.ncbi.nlm.nih.gov/BLAST/ , BIOEDIT Sequence Alignment Editor software publicly available at *http://www.mbio.ncsu.edu/BioEdit/BioEdit.html* and ClustalW algorithm provided by EMBL-EBI at *http://www.ebi.ac.uk/Tools/clustalw2/index.html*.

Another database used in this study is OncoDB.HCC- Oncogenomic Databas of Hepatocellular Carcinoma (Jou *et al.,* 2007) For querying name of ROBO-SLIT family

member genes were typed in the ‘Gene description’ section of ‘Display queried gene and reginal data’ query tool and ‘region around gene option’ on the left side of the query tool was left as default, +/- 10 Mb (megabases). On the return page, clicking on ‘display region’ gives information on the mapped human markers and LOH (loss of heterozygosity) regions around the queried gene.

For enhancer and promoter analysis GENOMATIX,CORG and PromoterScan softwares were used. The search algoritm was set to default in all parameters. Results of the putative promoter and enhancer sequences were listed according to their Z-score with the possible transcription factors.

For CpG island prediction analysis, EMBOSS CpG Plot software was used. All the parameters were set to default.

3.6 Sequencing of Constructs:

We have F1-pGL3, F2-pGL3, F3-pGL3, F4-pGL3 constructs sequenced in Iontek Inc (Istanbul, Turkey) by providing the company with PCR products and primers. Representative F1-pGL3 sequencing results were at the appendices part. To sequence F1, F2, F3 constructs F4, GL, and RV primers were used. For F4 construct GL and RV primers were used. For sequencing primers see the table 3.1

CHAPTER 4 RESULTS

4.1 Identification of ROBO-SLIT Family Genes Methylation Status and Expression Patterns:

4.1.1 Mutation Database Scanning of ROBO-SLIT Family:

Our group recently showed that members of ROBO-SLIT family of genes have different expression pattern in hepatocellular carcinoma cell lines (Avci ME et al. 2008). This differential expression might be due to either genetic mutations, and/or the change in the epigenetic control mechanisms of these genes. To check the first possibility the Human Genetic Mutation Database was scanned for the Small/ Gross Deletions, Small/ Gross Insertions type mutations for *ROBO1, ROBO2, ROBO3, ROBO4, SLIT1, SLIT2,* and *SLIT3* genes. No results were found for these types of mutations in Hepatocellular Carcinoma. Also OncoDB.HCC Database was scanned for the same mutation types and no such abnormalities could be found. Therefore, we turned out to study the methylation of *SLIT-ROBO* genes. As mentioned in the introduction part, SLIT ROBO family members were shown to be regulated by hypermethylation in different cancer types but, except *SLIT2*, this is never tested in HCC. Also, there is only one study that described *ROBO2* methylation in head and neck squamous carcinoma. On the other hand, ROBO1 is upregulated in liver cancer and ROBO4 expression was repeatedly shown to be confined to vascular endothelium. Hence, the focus of this study is to explore the epigenetic regulation of *ROBO2, ROBO3, SLIT1* and *SLIT3* in HCC.

4.1.2 Identification of ROBO2 Gene Regulatory Sequences:

Although *ROBO2* gene has very important roles in the development of kidney, and guidance of commissural axons, its promoter and enhancer sequences were not identified. Minus 10kb of Robo2 gene translation start site (TSS) sequence were retrieved from ENSEMBL Genome Browser Database. This sequence was scanned for the presence of both putative promoter and CpG Island presence. CpG Island Analysis was performed by Emboss CpG Plot website (**Figure 4.1**). A CpG Island was found to be located in the -1482 to -621 bp relative to TSS (**Figure 4.2**). Promoter Analysis was performed by "Promoter Scan" software developed by Bioinformatics and Molecular Analysis Section of NIH. Putative promoter region was found to be located in the -1343 to 1043 bp relative to TSS (**Figure 4.3**). This region have

strong promoter prediction score and high number of possible transcription factor binding sites (**Figure 4.2**).

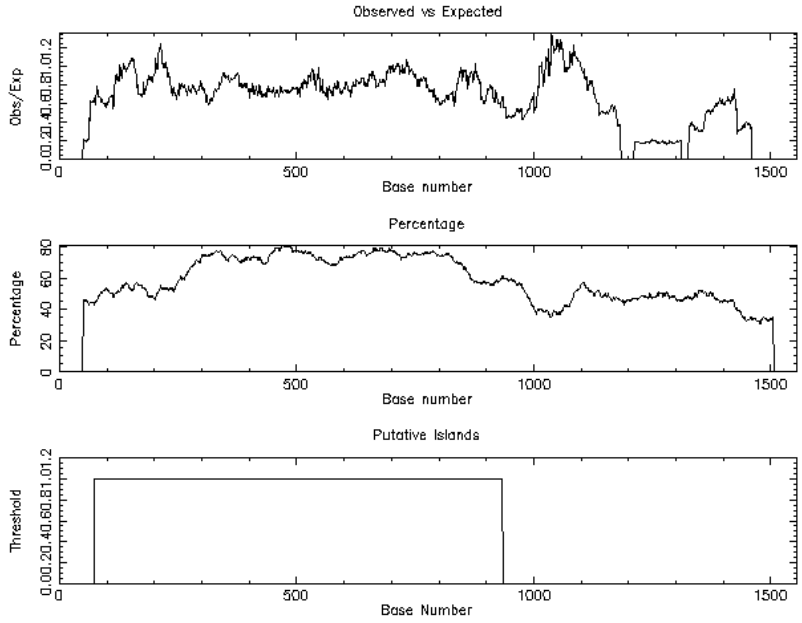

Figure 4.1

CpG Prediction Plot of Robo2 Gene. CpG Island was found to be located in the -1482 to -621 bp relative to TSS

Significant Signals:

Name	TFD #	Strand	Location	Weight
TTR_inverted_repeat	S01112	-	263	3.442000
AP-2	S01936	+	291	1.108000
JCV_repeated_sequenc	S01193	-	298	1.658000
Sp1	S00781	+	301	3.191000
Sp1	S00801	-	306	3.119000
T-Ag	S00974	+	323	1.086000
AP-2	S01936	-	326	1.091000
GCF	S01964	-	329	2.284000
UCE.2	S00437	-	364	1.216000
GCF	S01964	+	376	2.361000
NF-kB	S01498	+	378	1.080000
APRT-mouse_US	S00216	-	382	7.604000
AP-2	S00346	+	405	1.355000
AP-2	S01936	+	406	1.108000
AP-2	S01936	-	415	1.091000
JCV_repeated_sequenc	S01193	-	441	1.658000
Sp1	S00978	+	453	3.013000
Sp1	S00781	+	454	3.191000
Sp1	S00802	-	458	3.061000
Sp1	S00801	-	459	3.119000
UCE.2	S00437	+	461	1.278000
GCF	S01964	+	487	2.361000
AP-2	S00346	+	499	1.355000
EGR-1	S01956	+	500	5.736000
KROX24	S01624	+	500	9.559000
AP-2	S01936	+	502	1.108000
Sp1	S00956	+	502	9.386000
(Sp1)	S01187	+	503	8.117000
EARLY-SEQ1	S01081	+	503	6.322000
Sp1	S00801	+	504	2.755000
Sp1	S00802	+	505	3.292000
KROX24	S01623	-	508	5.378000
Sp1	S00781	-	509	2.772000
Sp1	S00978	-	510	3.361000
Sp1	S00326	-	511	9.386000
Sp1	S00979	-	511	6.023000
AP-2	S00180	+	513	1.863000

Figure 4.2

ROBO2 putative promoter predicted transcription factor binding sites and their binding probabilities

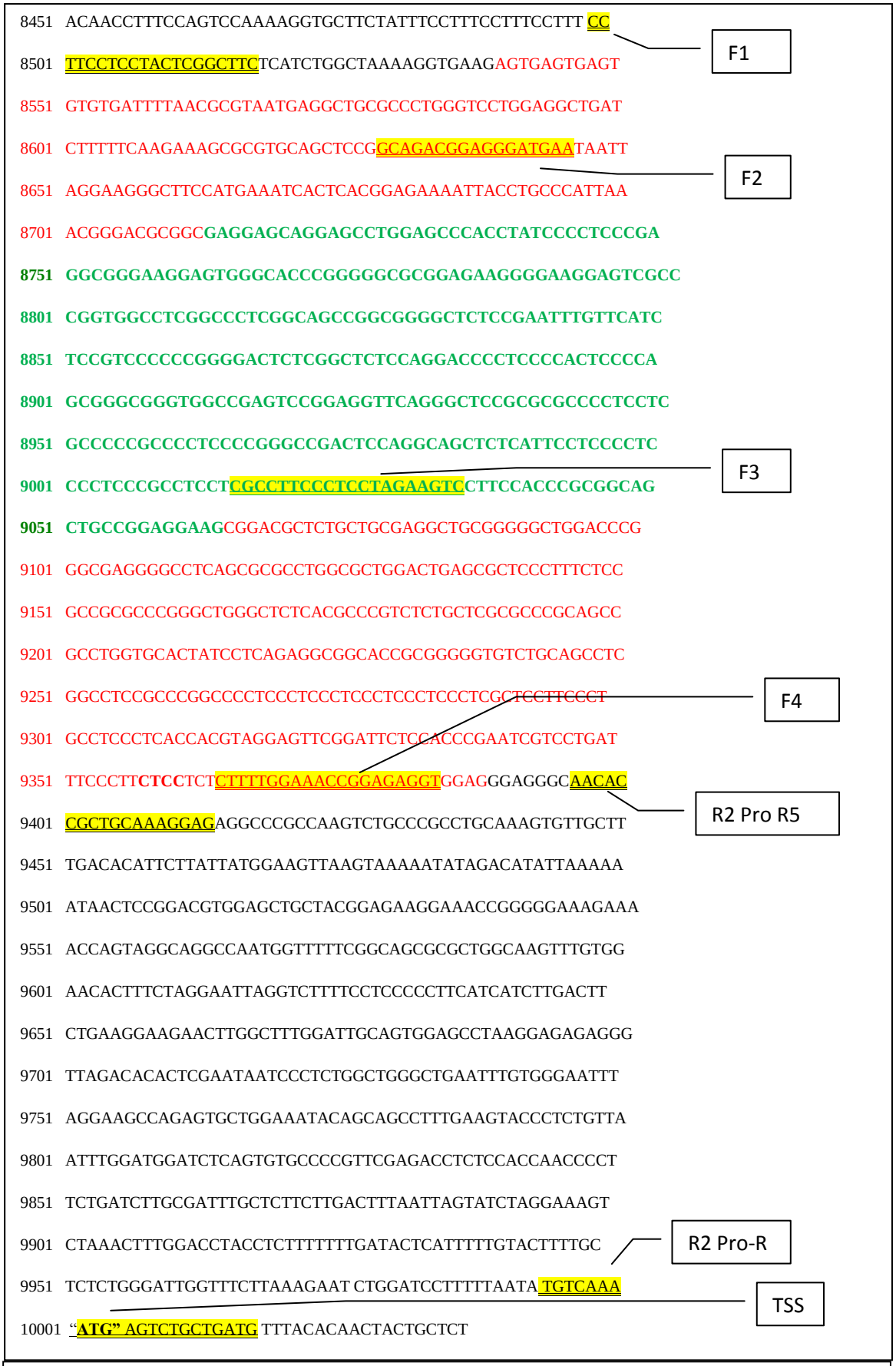

Figure 4.3 Localization of *ROBO2* primers in the putative promoter region that covers approximately -1600bp downstream of *ROBO2* TSS. TSS located at the 10000. Red Region is the putative CpG island and the Green region is the putative promoter.

4.1.3 Putative Promoter Site is Evolutionary Conserved

As mentioned above a putative promoter sequence for *ROBO2* was found with PromoterScan algorithm. It is located in the middle of a CpG island. It gives a high score for potential binding sites of transcription factors. This sequence is validated by also other databases (GENOMATIX, CORG) and all returned with high scores for a potential promoter. This putative promoter region is compared with ClustalW algorithm for interspecies conservation analysis. -10kb region of D*rosophila melanogaster*, *Mus musculus, and* -2kb region of *Human* sequence were analyzed by ClustalW algorithm.

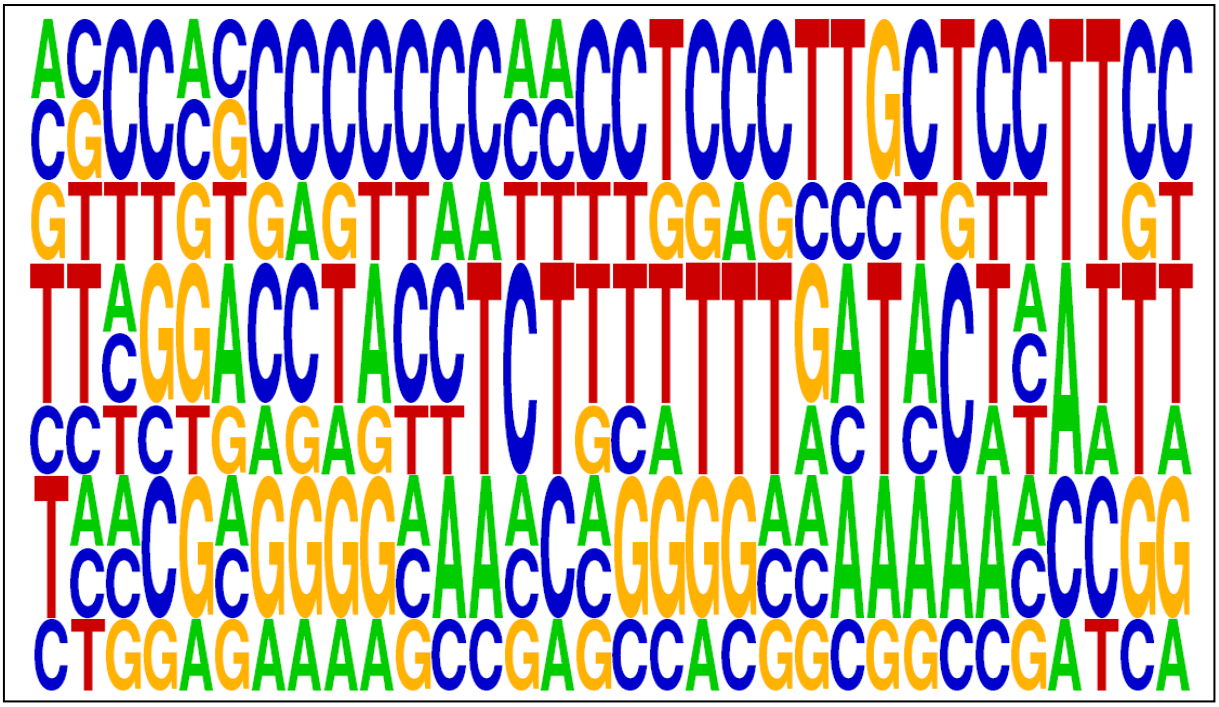

Figure 4.4: Representative part from the CLUSTALW algorithm comparison of Human, Mus Musculus and Drosophila *Robo2* upstream sequences

Mus musculus and Human sequences showed strong similarities in the whole sequence where as *Drosophila Melanogaster* showed less similarity. However, in the CpG island and promoter regions all three species showed strong similarity. (**Figure 4.6**) This putative region does not contain a significant TATA box. It has got potential binding sites for AP2 (8 times), SP1 (9 sites), NF-kB, APRT, JCV, GCF, EGR-1, KROX24 (2 times).

4.1.4 Identification of Putative CpG Islands of Other ROBO and SLIT Family Genes:

SLIT1, *SLIT3*, and *ROBO3* genes' upstream of TSSs were analyzed with Emboss CpG Plot. *SLIT1* has two putative CpG islands one of them is between -56 and -321 and the other one is -352 and -575 bp relative to the TSS. *ROBO3* has a CpG island located in -88 to -341.

SLIT 3 has CpG Island located between -126 and -817. Primers for Methylation Specific PCR of *SLIT 1*, *SLIT3* and *ROBO3* were previously reported (Narayan G. et al., 2006).

4.1.4 5-Aza-dC Treatment of HCC Cell Lines and Real Time PCR Analysis of ROBO-SLIT Family Genes in HCC Cell Lines:

HCC cell lines with high AFP background (Hep3B, PLC, Focus, Huh7) and low AFP expressing cells (SkHep1, HepG2, Snu387, and Snu423) were treated with 5-Aza-dC at 2.5μM concentration for 4 days. Total RNAs of these 5-Aza-dC treated and non treated cell lines were isolated and cDNA were prepared from these RNA. Real Time PCR analysis was performed with these cDNA to see that whether 5-Aza-dC treatment would have any effect on the expression patterns of ROBO-SLIT family members. Real Time PCR was performed in duplicates and transcript expression was normalized to *GAPDH*. Untreated cell lines were used as control.

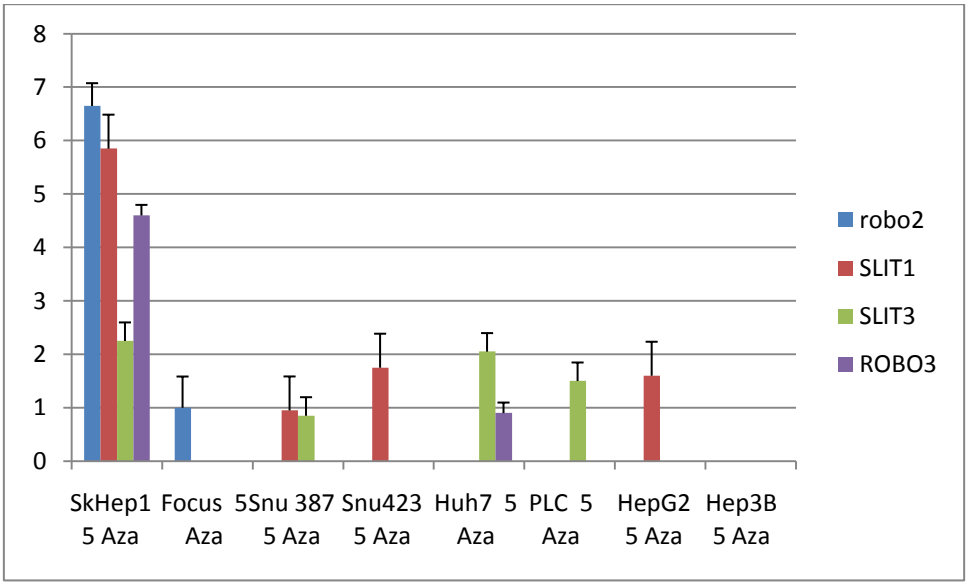

Figure 4.5 Real Time PCR Results of Expression patterns of *ROBO1, ROBO2, ROBO3, SLIT1* and *SLIT3* genes after 5-Aza-dC treatment of HCC cell lines. Results are in *log2* based and non-treated results are all equal zero. Normalization was performed according to *GAPDH*.

As shown in **Figure 4.4**, the expression of all analyzed genes (*ROBO2, ROBO3, SLIT1*, and *SLIT3*) increased in SkHep1 cell line, after 5-Aza-dC treatment. Snu387 showed an increase in *SLIT1* and *SLIT3*. HUH7 showed definite increment in the *SLIT3* and a slight increment in *ROBO3*. In PLC *SLIT3* was increased. Both HepG2 and Snu423 cell lines displayed an increment in *SLIT1* expression and Focus showed an increase in *ROBO2*. The

fact that *SLIT-ROBO* gene expression was rescued upon 5-Aza-dC treatment in HCC cell lines prompted us to study the methylation of their gene regulatory regions.

4.1.5 Bisulfite Treatment of HCC Cell Lines and MS-PCR

DNA of eight HCC cell lines (SKHep1, Focus, Snu387, Snu423, Huh7, PLC, HepG2, and Hep3B) was isolated and then subjected to bisulfite treatment. PCR reactions were run by using methylation-specific primers. Results were shown in **Figure 4.5**.

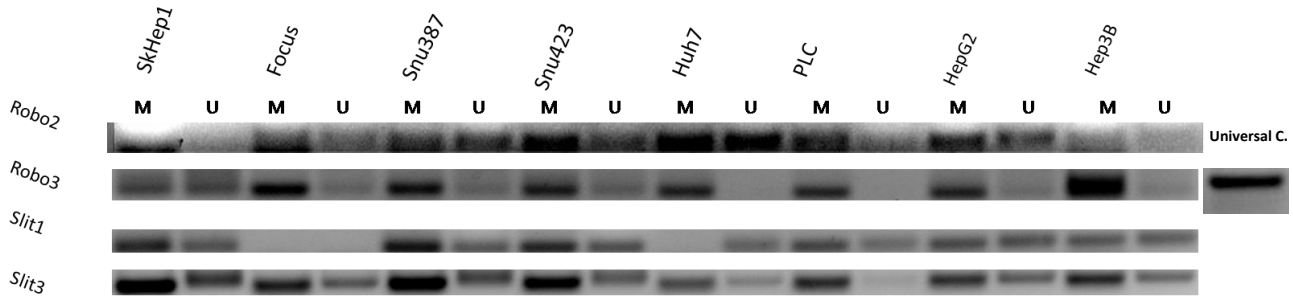

***Figure 4.6*:** Methylation Specific PCR of *ROBO2, ROBO3, SLIT1* and *SLIT3* genes. M means methylated form specific primer U means unmethylated specific form primer. Right most band is the control for the bisulifte treatment. Completely methylated human DNA (from Zymo Epigenetics) was subjected to bisulfite treatment and checked for presence of methylation for bHMLH primers and gave positive result.

Although *ROBO2* had a hemi-methylated pattern of methylation generally, Focus, Snu423, PLC and HepG2 displayed stronger methylated bands than the unmethylated ones. Except Skhep1, all cell lines were found to be methylated for *ROBO3*. The methylation was more evident in cell lines with high-AFP background. *SLIT1* shows a methylation pattern in the low-AFP HCC cell line group (SKHep1, Snu387, and Snu423) while it showed an unmethylated or hemi methylated pattern in the high-AFP HCC cell line group (Huh7, PLC, HepG2, Hep3B). No methylation of *SLIT1* was observed in Huh7 cells. With regard to *SLIT3* analysis, low-AFP group cell lines displayed strong methylated bands and concomitantly

present unmethylated bands, suggesting a hemi-methylated status of *SLIT3* in these cells. However, the absence of unmethylated PCR product in PLC and barely detectable band in HUH7 indicated a stronger methylation of *SLIT3* in cells with high-AFP expression.

4.2 Cloning of ROBO2 Gene Regulatory Sequences (Promoter &Enhancer):

4.2.1 Cloning of Different Fragments of Putative Promoter into pGL3 Luciferase Reporter Vector

To characterize this promoter, we designed 4 different forward primers (F1, F2, F3, and F4) and one reverse primer. Forward primers are positioned just at the beginning of the CpG island (F1-ROBO2), beginning of the promoter sequence and neglecting the first part of CpG island (F2-ROBO2), at the end of the promoter region (F3-ROBO2), and at the end of the CpG island (F4-ROBO2) (**Figure 4.3**). Reverse primer is located just at the beginning of the transcription start site. Forward primers contain *HindIII* restriction site and reverse primer contains an *NcoI* restriction site for cloning into pGL3 luciferase reporter vector (**Figure 4.7**). *NcoI* restriction site is located just at the beginning of the *luc* coding region (**Figure 4.8**).

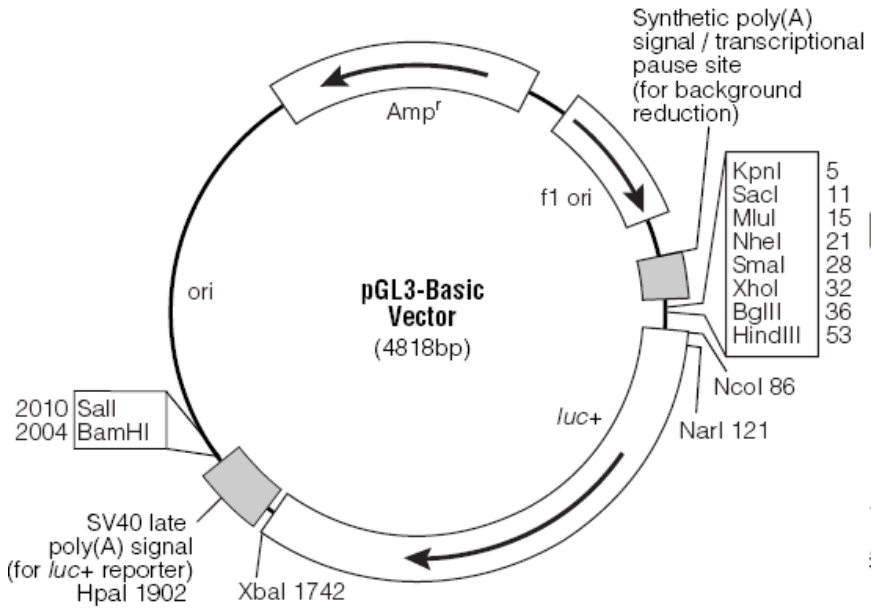

Figure 4.7: pGL3-Basic Vector circle map. *luc*+, cDNA encoding the modified firefly luciferase; Ampr, gene conferring ampicillin resistance in *E. coli*; f1 ori, origin of replication derived from filamentous phage; ori, origin of replication in *E. coli.* Arrows within *luc*+ and the Ampr gene indicate the direction of transcription; the arrow in the f1 ori indicates the direction of ssDNA strand synthesis. (PROMEGA Corporation, Technical Manual for pGL3 luciferase reporter vectors. Manual Code :TM033)

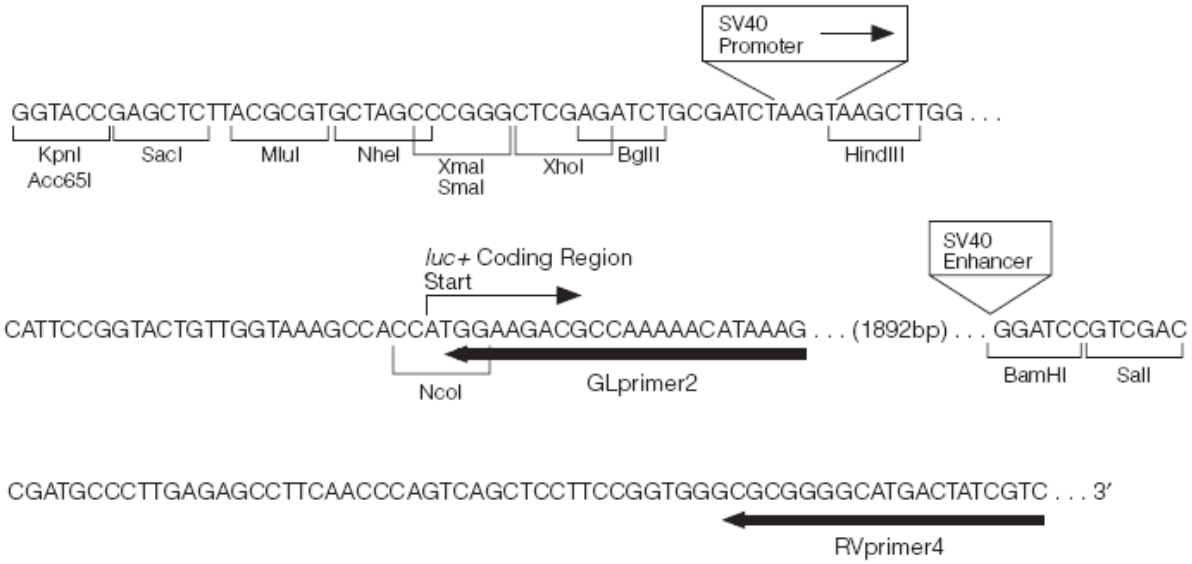

Figure 4.8: Multiple cloning site of pGL3 basic vector. *NcoI* is located just at the beginning of the TSS of *luc* gene. R2-PRO R sits just at that site. Forward primers contain *HindIII* restriction site at their 5' end. (PROMEGA Corporation, Technical Manual for pGL3 luciferase reporter vectors. Manual Code : TM033)

By using these primer pairs, we amplified 1502 bp, 1378 bp, 986 bp, and 636 bp products corresponding to F1, F2, F3 and F4, respectively (**Figure 4.9**).

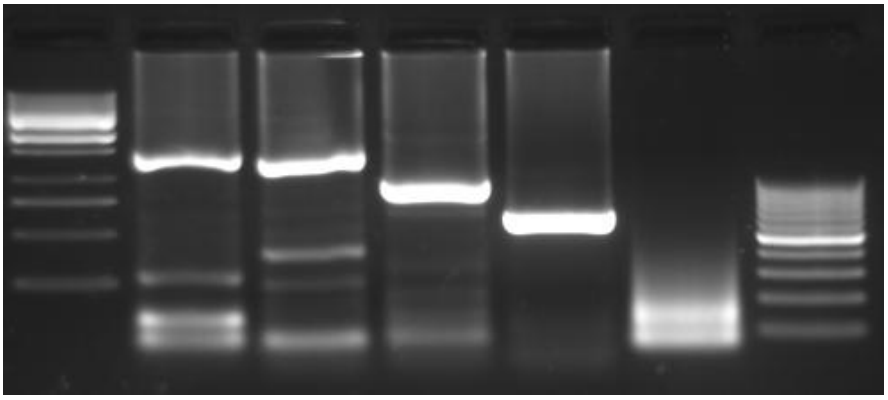

Figure 4.9: F1, F2, F3, and F4 inserts with sizes of 1502 bp, 1378 bp, 986 bp, and 636 bp respectively.

The aforementioned fragments were cut with *NcoI and HindIII* for cloning and run in 1% agarose gel. Cut inserts were isolated from the gel and ligated into the pGL3 vector. Plasmids were transformed into *E.coli* and Maxi Prep products were subjected to diagnostic restriction with the cloning enzymes (**Figure 4.10**). All products were at the right size. Vectors containing F1, F2, F3, and F4 inserts were named same as their inserts. F1, F2, F3, and F4 vectors were sequenced and no mutation was observed.

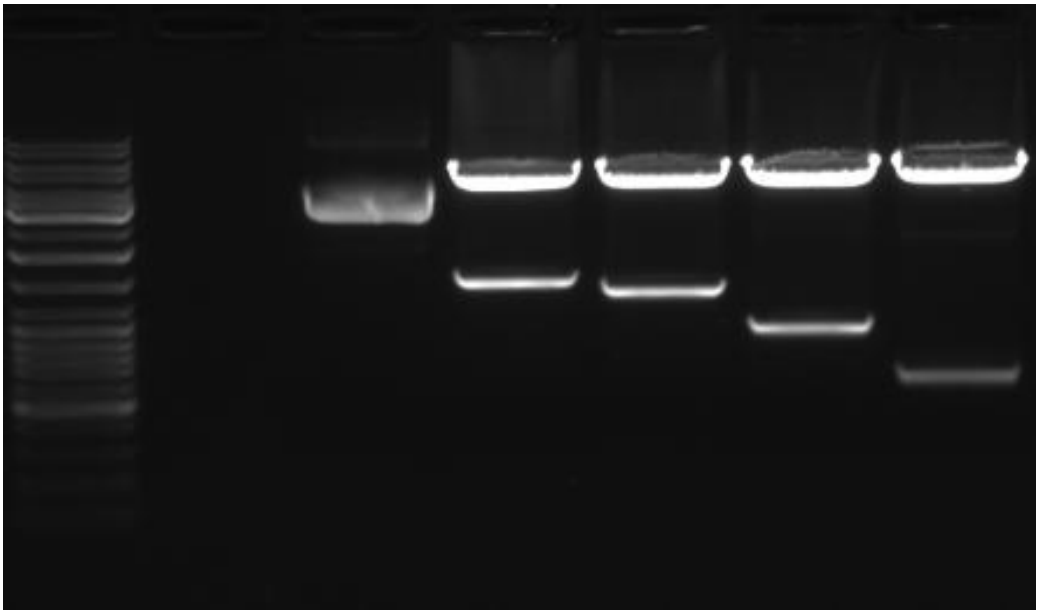

Figure 4.10: Diagnostic restriction cut of F1, F2, F3, and F4 vectors with NcoI and HindIII. Left band is the uncut pGL3 basic.

4.2.2 Luciferase Assay for F1, F2, F3, F4 vectors

Huh 7 cell line was selected for the transfection experiment since this cell line was previously shown to express *ROBO2* gene and suitable for transfection. F1-F4 constructs, CMV promoter driven luciferase vector, renilla TK, empty pGL3, and a GFP vector were transfected to Huh7 cells. All transfections were made in triplicate. 48 hours after the transfection cells were collected and lysed for luciferase assay with Promega Dual Glo Luciferase Kit. GFP transfected wells were checked for transfection efficiency. Luciferase signals were normalized according to renilla signals. The mean of the triplicate samples were taken and divided to the empty vector (pGL3) transfection intensities. Results are shown in **Figure 4.11**. All of the constructs gave lower signal than the empty vector (pGL3). This might be due to either:

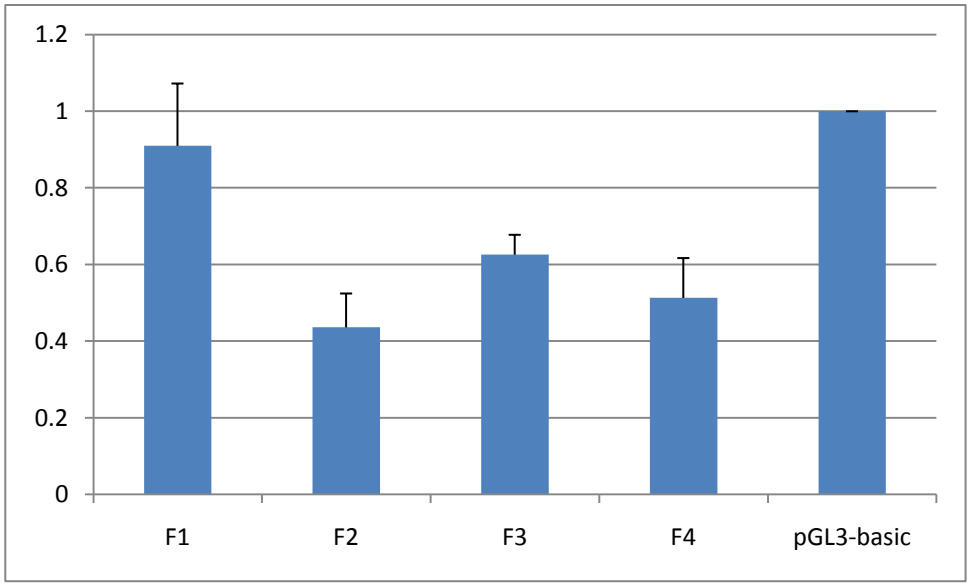

Figure 4.11: Luciferase assay results of F1, F2, F3, and F4 transfection. All transfections were made in triplicates. Non transfected wells' signals were accepted as background and subtracted from all of the results separately both for luciferase signals and renilla luciferase signals. Then luciferase signals were normalized according to renilla signals because renilla signals were the sign of transfection efficiency for each well. Then mean of the triplicate samples were taken and divided to the empty vector (pGL3-basic) transfection intensities.

i. Since *ROBO2* is a gene that functions in development it may need extra activating sequences (like an enhancer) additional to promoter. AND/OR,

ii. Putative promoter of *ROBO2* gene does not contain a TATA box and for this reason it is hard to provoke the sequence act as a promoter. AND/OR,

iii. There is/are strong repressor binding sites in this region and therefore putative promoter could not act in full capacity.

All of these possible reasons seem to act together and they all sourced from the functional nature of *ROBO2* gene. As being a gene regulating developmental processes, it might be subjected to strict regulation and it needs a complex mechanism to be transcribed.

At that time, Geisen MJ and colleagues showed that mouse *Robo2* is a direct target of Hoxa2 (Geisen MJ. et al., 2008). Binding region of Hoxa2 was also shown as a putative enhancer for *Robo2* gene by GENOMATIX database. This region covers 602 bp and located in intron1 (**Figure 4.12**). 2 sets of primers (Enhancer-Wide F/R & True Enhancer F/R) were designed for that region including the nested PCR primers. Primers contain *SalI* and *BamHI* restriction sites which are

ACATAAAATTAAGTAAAAAAAAATGGGTAGATATCTCAAACACTTAAGAGAAGA CCATTG

GAGAAAACCTCAAAAAATTGATAAATAAATAGTTTGCAACAATTAATAATGACAGTCTTT

GTATTTAAGAAAAAAAATCAGGTAGACATCTTTCCATACATGAAGTTAAAATAAT CATGG

GAATATTGAGTCCTTATCAA[ATCATAGCTTAAGTGGGAAAATCTAGGTAATACATATGTG

TGAAAGTACACATTTTTTGGTTTTCTCTAGCATTCTTGAGGAATATTAATATTTGTTTTT

TAAATGTTTTTATCCCTTTCAACTTTTAGTTTTCCCACTTTGAACCCTGATAATAGATTA

TTGTAATCATTTTTAATCTCTCTTTTTCCTGTAGAATTCAGTGTTCTGATTTTTTATGAT

AGGATCCACCTGATTTAGCTCAGGGATTCACTGAAAAATCAATTTAATATTTTTTTCCAA

AGGTTGTATGGTCTTATGTGCAAACTGTAGCTATTCCTTTGTTCCAAAATATCTTATTTT

ATTGAATGACATTGGATTCACAAGGCCTTATTAAAACACAGCTGAGGTACAGAGTTAGGT

ACCTGTGTACCAAAAGTAAATTAGGTTTCCTTTGCTTTTTTCATAATGTACTTAAAGCAT

GCATAATAGTTTATCTCATTTTACCATTGTTTCATTTTTTTTTTCAAGAACGACCCACAT

TTCTCAGGAGGCCAATTAACCAGGTGGTACTGGAGGAAGAAGCTGTAGAATTTCGTTGTC

AAGTCCAAGGAGATCCTCAACC]AACTGTGAGGTGGAAAAAGGATGATGCAGACTTGCCAA

GAGGAAGG TAAGACCAACATATGGATGGAAGATTGTTAGATAACCAATGAATAATTAGAA

AATAAA AGGACAGCTACAATGCCACCACC AAACACTCCTATGTCTTGGGGTACTTTCACT

Figure 4.12: Putative enhancer region of ROBO2 gene located in the first intron. Red region shows the enhancer. Green highlighted regions are True Enhancer F&R primers. Cyan highlighted ones are nested PCR primers Enhancer Wide F&R.

present in the pGL3 basic vector just before the enhancer site of pGL3 enhancer vector. Putative enhancer region was amplified from the product of the nested PCR (**Figure 4.13**).

To solve the TATA box problem a modified version of pGL3 vector (e1b-pGL3) was used which contains an e1b TATA box just before the *XhoI* restriction site in the multiple cloning site of the vector. New set of primers, which contain *MluI* and *XhoI* restriction sites, were designed for cloning the F1, F2, F3, and F4 regions after the e1b TATA box (F1 e1b, F2 e1b, F3 e1b, and F4 e1b) (**Figure 4.13**).

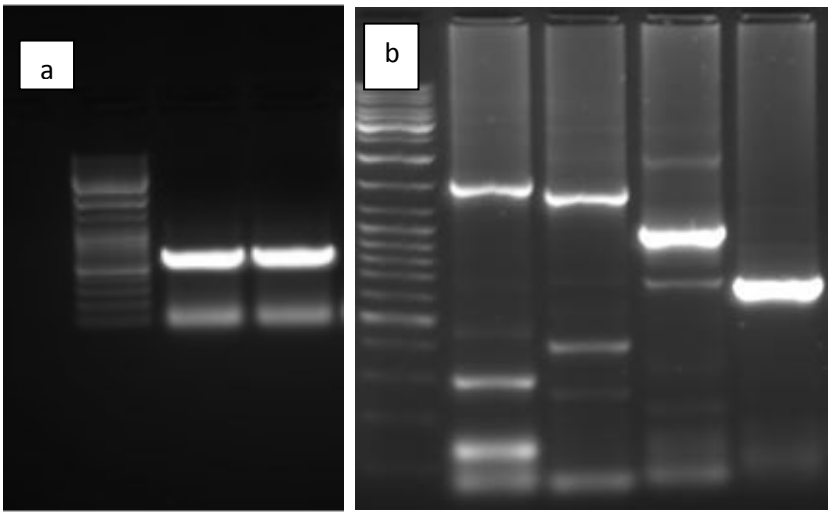

Figure 4.13: (a) Putative enhancer region of *ROBO2* gene with 602 bp size.

(b) Inserts F1, F2, F3, and F4 for e1b, which contain *MluI and XhoI* restriction sites at their ends.

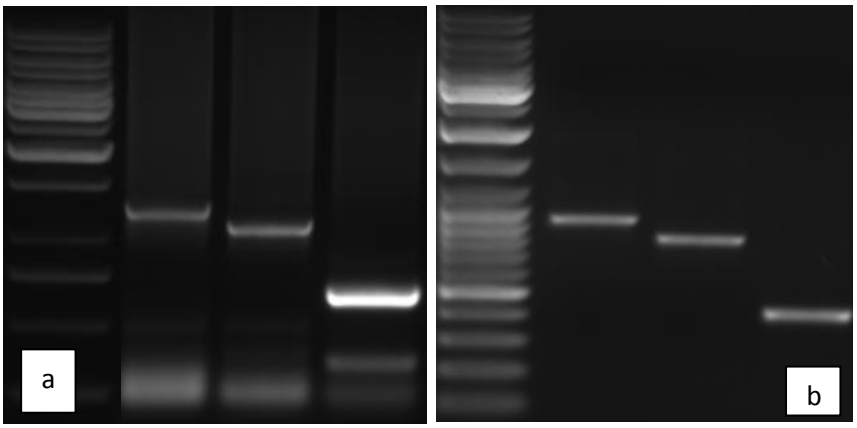

Figure 4.14: (a) F1-F4, F2-F4, F3-F4 for e1b vector.

(b)F1-F4, F2-F4, F3-F4 for pGL3 vector

To explore whether putative promoter region contains repressor binding sites, we scanned for possible repressors with different TF binding site predictors. 7 possible (IRF8, Nf-1, Oct1, GR1-alpha, Pu.1, NKX2-5, YY1) transcriptional repressor binding sites were found in F4 region. To minimize the effects of these possible repressors F4 region was excluded from the F1, F2, and F3 regions by designing two new reverse primers. One was for pGL3 and the other one was for e1b-pGL3 vector and they were located just downstream of the F4–F3 intersection (**Figure 4.2**). New inserts were named as F1-F4, F2-F4, F3-F4 (**Figure 4.14**), F1-F4 for e1b, F2-F4 for e1b, F3-F4 for e1b (**Figure 4.14**) and were synthesized from the nested PCR.

Putative enhancer insert has been ligated to both pGL3 basic and pGL3-e1b vector successfully. The cloning of F4 omitted inserts into 4 different vectors (pGL3-basic, pGL3+enhancer, pGL3-e1b, pGL3-e1b+ enhancer) was envisaged in order to reveal the potential of the putative promoter region as the gene regulatory site of *ROBO2* gene.

5. DISCUSSION AND FUTURE PERSPECTIVES:

Hepatocellular carcinoma is the fifth most common cancers worldwide and it is the third leading cause of cancer related deaths (Llovet JM. et al., 2003). Patients are often diagnosed at advanced stages of the disease when effective therapies are limited. In most cases, HCC develops on the basis of chronic hepatitis and cirrhosis, which in turn establish an environment of liver injury, inflammation and hepatocyte proliferation (Thorgeirsson SS and Grisham GW. et al., 2002). Therefore, understanding growth and survival pathways that influence hepatocarcinogenesis can reveal molecular components of this aggressive cancer and help to develop more efficient diagnostic and prognostic tools and novel therapeutic targets as well.

Our group previously showed differential expression of *SLIT-ROBO* genes in HCC. (Avci ME et al. 2008). In the present study, we explored the epigenetic regulation of this family of genes in eight HCC cell lines, with a special focus on their methylation pattern. *ROBO1* was previously shown to be overexpressed in HCC (Ito H., et al., 2006). More recently, *SLIT2* inactivation in liver cancer by hypermethylation was also defined (Jin J. et al., 2009). On the other hand, several reports indicated vascular endothelium limited expression of *ROBO4*. Hence, we limited our methylation analyses to *SLIT1*, *SLIT3*, *ROBO2* and *ROBO3* genes whose methylation was never studied in HCC.

Initially, we treated cell lines by 5-Aza-dC to assess whether transcription of *SLIT-ROBO* genes can be rescued. However, we obtained only partial gene expression response of cell lines under our treatment conditions. For instance, we treated SkHep1 cells with 2.5 μM for 2 days and 4 days and also with 5μM for the same time scale. Then we evaluated the expression of *ROBO3* by Real Time PCR and observed that cells treated with 2.5 μM of 5-Aza-dC for 4 days displayed increased *ROBO3* expression. In fact, lower doses of drug treatment was safer than higher doses, since drug concentrations beyond 5 μM appeared to be toxic and led to cell death. However, some groups treated cells with 10 μM for 10 days (Fan H. et al., 1996), and accordingly, our dose could not be enough to relieve all the methylation in the genome. Nevertheless, this partial response led us to study the hypermethylation of aforementioned *SLIT-ROBO* genes.

Unlike partial response that cells displayed under our treatment conditions, all HCC cell lines were shown to have methylated *SLIT-ROBO* genes with a few exceptions. The most striking methylation pattern was observed in *ROBO3* gene, which was heavily methylated in all cell lines except SkHep1. This latter displayed hemi-methylation, yet in Real-Time PCR

analysis, 5-Aza-dC treated cells showed a 4.6 fold increase in *ROBO3* expression when compared to untreated cells. Also Huh7 cell displayed a slight increase near to 2 fold. In other cell lines treated with 5-Aza-dC, no *ROBO3* amplification was observed with three different sets of primers. This was most likely due to low dose treatment conditions, but also indicated that *ROBO3* gene regulatory region is heavily methylated. Cell lines that were selected for methylation analysis also cover the high-AFP expressing well differentiated and low-AFP expressing poorly differentiated stages of HCC. Therefore, fully methylated pattern of *ROBO3* in all cell lines suggests that the inactivation of *ROBO3* is an early event in hepatocarcinogenesis. It was recently shown that ROBO3 represses ROBO1, which was also shown to be overexpressed in HCC (Sabatier C. et al., 2004). Our results are in accordance with this finding and implicate a possible role of ROBO1-ROBO3 axis in HCC development. There are only few studies describing *ROBO3* methylation in human cancers. One report demonstrated the inactivation of *ROBO3* by hypermethylation in cervical cancer (Narayan G et al. 2006). However, in the same study *ROBO1* promoter region was also shown to be methylated. Thus, opposite behavior of *ROBO1* and *ROBO3* appears to occur only in liver cancer and it is worthy to examine *ROBO3* role as a potential tumor suppressor gene in HCC

Both methylation and hemi-methylation of *SLIT1* were observed. Also low-AFP expressing SkHep1, Focus, Snu387, and Snu423 had got stronger methylation pattern than the high-AFP expressing PLC, HepG2, Hep3B and Huh7. These results were in accordance with our previous findings that *SLIT1* expression was more obvious in HCC cell lines with high-AFP background (Avci ME et al. 2008). In this previous observation, *SLIT3* expression was found to be confined to low-AFP group of cell lines. The methylation analysis confirmed this pattern of gene expression in that high-AFP cells had barely detectable unmethylated DNA amplification.

ROBO2 had a hemimethylated pattern in HCC cell lines, yet this was more obvious in high-AFP expressing cells. In other words, low-AFP group of cells displayed heavier methylation. This finding validates our previous results showing *ROBO2* expression in HCC cell lines of high-AFP group. To our best knowledge, *ROBO2* methylation was only studied in head and neck squamous carcinoma (Ghosh S. et al., 2009). The limited data on epigenetic regulation of *ROBO2* is most probably due to the lack of knowledge about its gene regulatory sequence. Hence, this study also targeted to identify the promoter of *ROBO2* gene given that our methylation specific primers were designed from the CpG island that covers the putative promoter sequence.

Since MS-PCRs were performed in 45 cycles, it was a high probability that the reactions have reached the saturation plateau. For this reason quantitative analysis should be performed in order to establish a reliable connection between the expression pattern panel and MS-PCR. Also there may be transcriptional regulation mechanisms other than CpG methylation that have a role in the regulation of these genes. So it is hard to say that there is 100% correlation between the MS-PCR and expression panel but it is obvious that there is a strong relation between these two.

Promoter prediction analysis of *ROBO2* initially gave high prediction score and high transcription factor binding probabilities. The potential of this region as a gene regulatory site was also validated by the presence of a CpG island that covers the putative promoter region. Several fragments corresponding to this region were cloned into pGL3-basic luciferase vector. However our initial experiments failed to work because of the inherent features of this putative promoter. Since ROBO2 takes role in the developmental processes, it might have complex transcriptional control mechanisms than the other genes that are controlled basically on their close proximity promoter. Lack of a TATA box in the close proximity of the TSS supports that hypothesis. The absence of a TATA box led us to clone promoter fragments into TATA box containing reporter vector along with an enhancer, which is located in the first intron of *ROBO2*. Furthermore, analysis of the F4 promoter fragment also revealed a potential repressor binding site. Therefore we also envisaged to omit this region from previously cloned fragments.

Herein, we described the methylation of *SLIT-ROBO* genes in hepatocellular carcinoma cell lines and found out that this pathway is regulated in this cancer. Fully methylated pattern of *ROBO3* gene might give insight into the identification of a new pathway in liver cancer, taken together with the overexpression of *ROBO1*, which is confined to HCC.

Future Perspectives:

Planned future works are as follows:

(i) Extending methylation studies to HCC patients in order to explore whether our cell line data translate into in vivo conditions.

(ii) Functional studies with *ROBO3* gene that will deal with the transfection of *ROBO3* into HCC cell lines and assess their phenotype thereof.

(iii) To design new reporter assays that will take into account the inherent properties of *ROBO2* gene regulatory sequence.

(iv) TSA treatment additional to 5-Aza-dC treatment may help to relieve the epigenetic pressure, especially on *ROBO3* gene.

References:

Agirre, X., F. J. Novo, et al. (2003). "TP53 is frequently altered by methylation, mutation, and/or deletion in acute lymphoblastic leukaemia." Mol Carcinog **38**(4): 201-8.

Avci, M. E., O. Konu, et al. (2008). "Quantification of SLIT-ROBO transcripts in hepatocellular carcinoma reveals two groups of genes with coordinate expression." BMC Cancer **8**: 392.

Bachman, K. E., J. G. Herman, et al. (1999). "Methylation-associated silencing of the tissue inhibitor of metalloproteinase-3 gene suggest a suppressor role in kidney, brain, and other human cancers." Cancer Res **59**(4): 798-802.

Bacolla, A., S. Pradhan, et al. (1999). "Recombinant human DNA (cytosine-5) methyltransferase. II. Steady-state kinetics reveal allosteric activation by methylated dna." J Biol Chem **274**(46): 33011-9.

Battye, R., A. Stevens, et al. (1999). "Axon repulsion from the midline of the Drosophila CNS requires slit function." Development **126**(11): 2475-81.

Bestor, T. H. (2000). "The DNA methyltransferases of mammals." Hum Mol Genet **9**(16): 2395-402.

Bestor, T. H. (2000). "The DNA methyltransferases of mammals." Hum Mol Genet **9**(16): 2395-402.

Bosch FX, Ribes J, Cleries R, Diaz M. 2005. Epidemiology of hepatocellular carcinoma. Clinics in liver disease 9:191-211, v

Brena, R. M., H. Auer, et al. (2006). "Accurate quantification of DNA methylation using combined bisulfite restriction analysis coupled with the Agilent 2100 Bioanalyzer platform." Nucleic Acids Res **34**(3): e17.

Brose, K., K. S. Bland, et al. (1999). "Slit proteins bind Robo receptors and have an evolutionarily conserved role in repulsive axon guidance." Cell **96**(6): 795-806.

Carnell, A. N. and J. I. Goodman (2003). "The long (LINEs) and the short (SINEs) of it: altered methylation as a precursor to toxicity." Toxicol Sci **75**(2): 229-35.

Charron, F., E. Stein, et al. (2003). "The morphogen sonic hedgehog is an axonal chemoattractant that collaborates with netrin-1 in midline axon guidance." Cell **113**(1): 11-23.

Dallol, A., E. Forgacs, et al. (2002). "Tumour specific promoter region methylation of the human homologue of the Drosophila Roundabout gene DUTT1 (ROBO1) in human cancers." Oncogene **21**(19): 3020-8.

Dallol, A., D. Krex, et al. (2003). "Frequent epigenetic inactivation of the SLIT2 gene in gliomas." Oncogene **22**(29): 4611-6.

Dallol, A., D. Morton, et al. (2003). "SLIT2 axon guidance molecule is frequently inactivated in colorectal cancer and suppresses growth of colorectal carcinoma cells." Cancer Res **63**(5): 1054-8.

Das, P. M. and R. Singal (2004). "DNA methylation and cancer." J Clin Oncol **22**(22): 4632-42.

Dickinson, R. E., A. Dallol, et al. (2004). "Epigenetic inactivation of SLIT3 and SLIT1 genes in human cancers." Br J Cancer **91**(12): 2071-8.

Dickson, B. J. and G. F. Gilestro (2006). "Regulation of commissural axon pathfinding by slit and its Robo receptors." Annu Rev Cell Dev Biol **22**: 651-75.

Esteller, M., J. M. Silva, et al. (2000). "Promoter hypermethylation and BRCA1 inactivation in sporadic breast and ovarian tumors." J Natl Cancer Inst **92**(7): 564-9.

Fan, X., J. P. Labrador, et al. (2003). "Slit stimulation recruits Dock and Pak to the roundabout receptor and increases Rac activity to regulate axon repulsion at the CNS midline." Neuron **40**(1): 113-27.

Geiman, T. M., U. T. Sankpal, et al. (2004). "DNMT3B interacts with hSNF2H chromatin remodeling enzyme, HDACs 1 and 2, and components of the histone methylation system." Biochem Biophys Res Commun **318**(2): 544-55.

Geisen, M. J., T. Di Meglio, et al. (2008). "Hox paralog group 2 genes control the migration of mouse pontine neurons through slit-robo signaling." PLoS Biol **6**(6): e142.

Ghosh S, Ghosh A, Maiti GP, Alam N, Roy A, Roychoudhury S, Panda CK: Alterations of ROBO1/DUTT1 and ROBO2 loci in early dysplastic lesions of head and neck: clinical and prognostic implications. *Human genetics* 2009, 125(2):189-198.

Graff, J. R., J. G. Herman, et al. (1995). "E-cadherin expression is silenced by DNA hypermethylation in human breast and prostate carcinomas." Cancer Res **55**(22): 5195-9.

Grieshammer, U., M. Le, et al. (2004). "SLIT2-mediated ROBO2 signaling restricts kidney induction to a single site." Dev Cell **6**(5): 709-17.

Hendrich, B. and A. Bird (1998). "Identification and characterization of a family of mammalian methyl-CpG binding proteins." Mol Cell Biol **18**(11): 6538-47.

Holmes, G. P., K. Negus, et al. (1998). "Distinct but overlapping expression patterns of two vertebrate slit homologs implies functional roles in CNS development and organogenesis." Mech Dev **79**(1-2): 57-72.

http://www.hgmd.cf.ac.uk/ac/all.php

http://www.ensembl.org/index.html

http://www.ebi.ac.uk/Tools/emboss/cpgplot/

http://www-bimas.cit.nih.gov/molbio/proscan/

http://www.ebi.ac.uk/Tools/clustalw2/index.html

Hsiao, W. L., G. Mendosa, et al. (1996). "Comparison of transformation by manganese sulfate and 5-azacytidine in Rat 6 cells overexpressing the c-myc oncogene." Carcinogenesis **17**(12): 2771-7.

Hu, H., M. Li, et al. (2005). "Cross GTPase-activating protein (CrossGAP)/Vilse links the Roundabout receptor to Rac to regulate midline repulsion." Proc Natl Acad Sci U S A **102**(12): 4613-8.

Huminiecki, L. and R. Bicknell (2000). "In silico cloning of novel endothelial-specific genes." Genome Res **10**(11): 1796-806.

Huminiecki, L., M. Gorn, et al. (2002). "Magic roundabout is a new member of the roundabout receptor family that is endothelial specific and expressed at sites of active angiogenesis." Genomics **79**(4): 547-52.

Hummel, T., K. Schimmelpfeng, et al. (1999). "Commissure formation in the embryonic CNS of Drosophila." Dev Biol **209**(2): 381-98.

Ito, H., S. Funahashi, et al. (2006). "Identification of ROBO1 as a novel hepatocellular carcinoma antigen and a potential therapeutic and diagnostic target." Clin Cancer Res **12**(11 Pt 1): 3257-64.

Ito H., A., T. Miyabayashi, et al. (1998). "Cloning and expressions of three mammalian homologues of Drosophila slit suggest possible roles for Slit in the formation and maintenance of the nervous system." Brain Res Mol Brain Res **62**(2): 175-86.

Jackson, J. P., A. M. Lindroth, et al. (2002). "Control of CpNpG DNA methylation by the KRYPTONITE histone H3 methyltransferase." Nature **416**(6880): 556-60.

Jin, J., H. You, et al. (2009). "Epigenetic inactivation of SLIT2 in human hepatocellular carcinomas." Biochem Biophys Res Commun **379**(1): 86-91.

Jones, C. A., N. R. London, et al. (2008). "Robo4 stabilizes the vascular network by inhibiting pathologic angiogenesis and endothelial hyperpermeability." Nat Med **14**(4): 448-53.
Jones, C. A., N. R. London, et al. (2008). "Robo4 stabilizes the vascular network by inhibiting pathologic angiogenesis and endothelial hyperpermeability." Nat Med **14**(4): 448-53.
Keleman, K., S. Rajagopalan, et al. (2002). "Comm sorts robo to control axon guidance at the Drosophila midline." Cell **110**(4): 415-27.

Kennedy, T. E., T. Serafini, et al. (1994). "Netrins are diffusible chemotropic factors for commissural axons in the embryonic spinal cord." Cell **78**(3): 425-35.

Kidd, T., K. S. Bland, et al. (1999). "Slit is the midline repellent for the robo receptor in Drosophila." Cell **96**(6): 785-94.

Kidd, T., K. Brose, et al. (1998). "Roundabout controls axon crossing of the CNS midline and defines a novel subfamily of evolutionarily conserved guidance receptors." Cell **92**(2): 205-15.

Kume, T., K. Deng, et al. (2000). "Murine forkhead/winged helix genes Foxc1 (Mf1) and Foxc2 (Mfh1) are required for the early organogenesis of the kidney and urinary tract." Development **127**(7): 1387-95.

Latil, A., L. Chene, et al. (2003). "Quantification of expression of netrins, slits and their receptors in human prostate tumors." Int J Cancer **103**(3): 306-15.

Li, H. S., J. H. Chen, et al. (1999). "Vertebrate slit, a secreted ligand for the transmembrane protein roundabout, is a repellent for olfactory bulb axons." Cell **96**(6): 807-18.

Liu, Z., K. Patel, et al. (2004). "Extracellular Ig domains 1 and 2 of Robo are important for ligand (Slit) binding." Mol Cell Neurosci **26**(2): 232-40.

Llovet JM, Burroughs A, Bruix J. 2003. Hepatocellular carcinoma. Lancet 362:1907-17

Long, H., C. Sabatier, et al. (2004). "Conserved roles for Slit and Robo proteins in midline commissural axon guidance." Neuron **42**(2): 213-23.

Luczak, M. W. and P. P. Jagodzinski (2006). "The role of DNA methylation in cancer development." Folia Histochem Cytobiol **44**(3): 143-54.
Luczak, M. W. and P. P. Jagodzinski (2006). "The role of DNA methylation in cancer development." Folia Histochem Cytobiol **44**(3): 143-54.
Lundstrom, A., M. Gallio, et al. (2004). "Vilse, a conserved Rac/Cdc42 GAP mediating Robo repulsion in tracheal cells and axons." Genes Dev **18**(17): 2161-71.

Melki, J. R., P. C. Vincent, et al. (1999). "Concurrent DNA hypermethylation of multiple genes in acute myeloid leukemia." Cancer Res **59**(15): 3730-40.

Moore, M. W., R. D. Klein, et al. (1996). "Renal and neuronal abnormalities in mice lacking GDNF." Nature **382**(6586): 76-9.

Mutskov, V. J., C. M. Farrell, et al. (2002). "The barrier function of an insulator couples high histone acetylation levels with specific protection of promoter DNA from methylation." Genes Dev **16**(12): 1540-54.

Narayan, G., C. Goparaju, et al. (2006). "Promoter hypermethylation-mediated inactivation of multiple Slit-Robo pathway genes in cervical cancer progression." Mol Cancer **5**: 16.

Pachnis, V., B. Mankoo, et al. (1993). "Expression of the c-ret proto-oncogene during mouse embryogenesis." Development **119**(4): 1005-17.

Pakneshan, P., M. Szyf, et al. (2005). "Methylation and inhibition of expression of uPA by the RAS oncogene: divergence of growth control and invasion in breast cancer cells." Carcinogenesis **26**(3): 557-64.

Piper, M., K. Georgas, et al. (2000). "Expression of the vertebrate Slit gene family and their putative receptors, the Robo genes, in the developing murine kidney." Mech Dev **94**(1-2): 213-7.

Piper, M., K. Georgas, et al. (2000). "Expression of the vertebrate Slit gene family and their putative receptors, the Robo genes, in the developing murine kidney." Mech Dev **94**(1-2): 213-7.

Piper, M., K. Georgas, et al. (2000). "Expression of the vertebrate Slit gene family and their putative receptors, the Robo genes, in the developing murine kidney." Mech Dev **94**(1-2): 213-7.

Prasad, A., A. Z. Fernandis, et al. (2004). "Slit protein-mediated inhibition of CXCR4-induced chemotactic and chemoinvasive signaling pathways in breast cancer cells." J Biol Chem **279**(10): 9115-24.

Prasad, A., V. Paruchuri, et al. (2008). "Slit-2 induces a tumor-suppressive effect by regulating beta-catenin in breast cancer cells." J Biol Chem **283**(39): 26624-33.

Reik, W. and W. Dean (2001). "DNA methylation and mammalian epigenetics." Electrophoresis **22**(14): 2838-43.

Rodriguez, J., J. Frigola, et al. (2006). "Chromosomal instability correlates with genome-wide DNA demethylation in human primary colorectal cancers." Cancer Res **66**(17): 8462-9468.

Rothberg, J. M., D. A. Hartley, et al. (1988). "slit: an EGF-homologous locus of D. melanogaster involved in the development of the embryonic central nervous system." Cell **55**(6): 1047-59.

Sabatier, C., A. S. Plump, et al. (2004). "The divergent Robo family protein rig-1/Robo3 is a negative regulator of slit responsiveness required for midline crossing by commissural axons." Cell **117**(2): 157-69.

Saxen, L. and H. Sariola (1987). "Early organogenesis of the kidney." Pediatr Nephrol **1**(3): 385-92.

Schimmelpfeng, K., S. Gogel, et al. (2001). "The function of leak and kuzbanian during growth cone and cell migration." Mech Dev **106**(1-2): 25-36.

Seeger, M., G. Tear, et al. (1993). "Mutations affecting growth cone guidance in Drosophila: genes necessary for guidance toward or away from the midline." Neuron **10**(3): 409-26.

Senolt, L., M. Grigorian, et al. (2006). "S100A4 (Mts1): is there any relation to the pathogenesis of rheumatoid arthritis?" Autoimmun Rev **5**(2): 129-31.

Serafini, T., T. E. Kennedy, et al. (1994). "The netrins define a family of axon outgrowth-promoting proteins homologous to C. elegans UNC-6." Cell **78**(3): 409-24.

Steele, W., C. Allegrucci, et al. (2005). "Human embryonic stem cell methyl cycle enzyme expression: modelling epigenetic programming in assisted reproduction?" Reprod Biomed Online **10**(6): 755-66.

Steele, W., C. Allegrucci, et al. (2005). "Human embryonic stem cell methyl cycle enzyme expression: modelling epigenetic programming in assisted reproduction?" Reprod Biomed Online **10**(6): 755-66.

Stirzaker, C., D. S. Millar, et al. (1997). "Extensive DNA methylation spanning the Rb promoter in retinoblastoma tumors." Cancer Res **57**(11): 2229-37.

Su, W. H., C. C. Chao, et al. (2007). "OncoDB.HCC: an integrated oncogenomic database of hepatocellular carcinoma revealed aberrant cancer target genes and loci." Nucleic Acids Res **35**(Database issue): D727-31.

Sundaresan, V., G. Chung, et al. (1998). "Homozygous deletions at 3p12 in breast and lung cancer." Oncogene **17**(13): 1723-9.

Szyf, M., P. Pakneshan, et al. (2004). "DNA methylation and breast cancer." Biochem Pharmacol **68**(6): 1187-97.

Tear, G., R. Harris, et al. (1996). "Commissureless controls growth cone guidance across the CNS midline in Drosophila and encodes a novel membrane protein." Neuron **16**(3): 501-14.

Thorgeirsson SS, Grisham JW. 2002. Molecular pathogenesis of human hepatocellular carcinoma. Nature Genetics **31**:339-46

Veigl, M. L., L. Kasturi, et al. (1998). "Biallelic inactivation of hMLH1 by epigenetic gene silencing, a novel mechanism causing human MSI cancers." Proc Natl Acad Sci U S A **95**(15): 8698-702.

Villar-Garea, A. and M. Esteller (2004). "Histone deacetylase inhibitors: understanding a new wave of anticancer agents." Int J Cancer **112**(2): 171-8.

Wade, P. A. (2001). "Methyl CpG-binding proteins and transcriptional repression." Bioessays **23**(12): 1131-7.

Walsh, C. P., J. R. Chaillet, et al. (1998). "Transcription of IAP endogenous retroviruses is constrained by cytosine methylation." Nat Genet **20**(2): 116-7.

Wang, B., Y. Xiao, et al. (2003). "Induction of tumor angiogenesis by Slit-Robo signaling and inhibition of cancer growth by blocking Robo activity." Cancer Cell **4**(1): 19-29.

Wang, K. H., K. Brose, et al. (1999). "Biochemical purification of a mammalian slit protein as a positive regulator of sensory axon elongation and branching." Cell **96**(6): 771-84.

Wang, Y., W. Fischle, et al. (2004). "Beyond the double helix: writing and reading the histone code." Novartis Found Symp **259**: 3-17; discussion 17-21, 163-9.

Weisenberger, D. J., M. Velicescu, et al. (2004). "Role of the DNA methyltransferase variant DNMT3b3 in DNA methylation." Mol Cancer Res **2**(1): 62-72.

Wong, K., X. R. Ren, et al. (2001). "Signal transduction in neuronal migration: roles of GTPase activating proteins and the small GTPase Cdc42 in the Slit-Robo pathway." Cell **107**(2): 209-21.

Wu, J. Y., L. Feng, et al. (2001). "The neuronal repellent Slit inhibits leukocyte chemotaxis induced by chemotactic factors." Nature **410**(6831): 948-52.

Xian, J., K. J. Clark, et al. (2001). "Inadequate lung development and bronchial hyperplasia in mice with a targeted deletion in the Dutt1/Robo1 gene." Proc Natl Acad Sci U S A **98**(26): 15062-6.

Yuan, W., L. Zhou, et al. (1999). "The mouse SLIT family: secreted ligands for ROBO expressed in patterns that suggest a role in morphogenesis and axon guidance." Dev Biol **212**(2): 290-306.

CHAPTER 6 APPENDICES

Appendix A Sequencing Results of F1, F2, F3, F4 Constructs

F1 Sequencing with RV3 primer which scans the first 500 bp

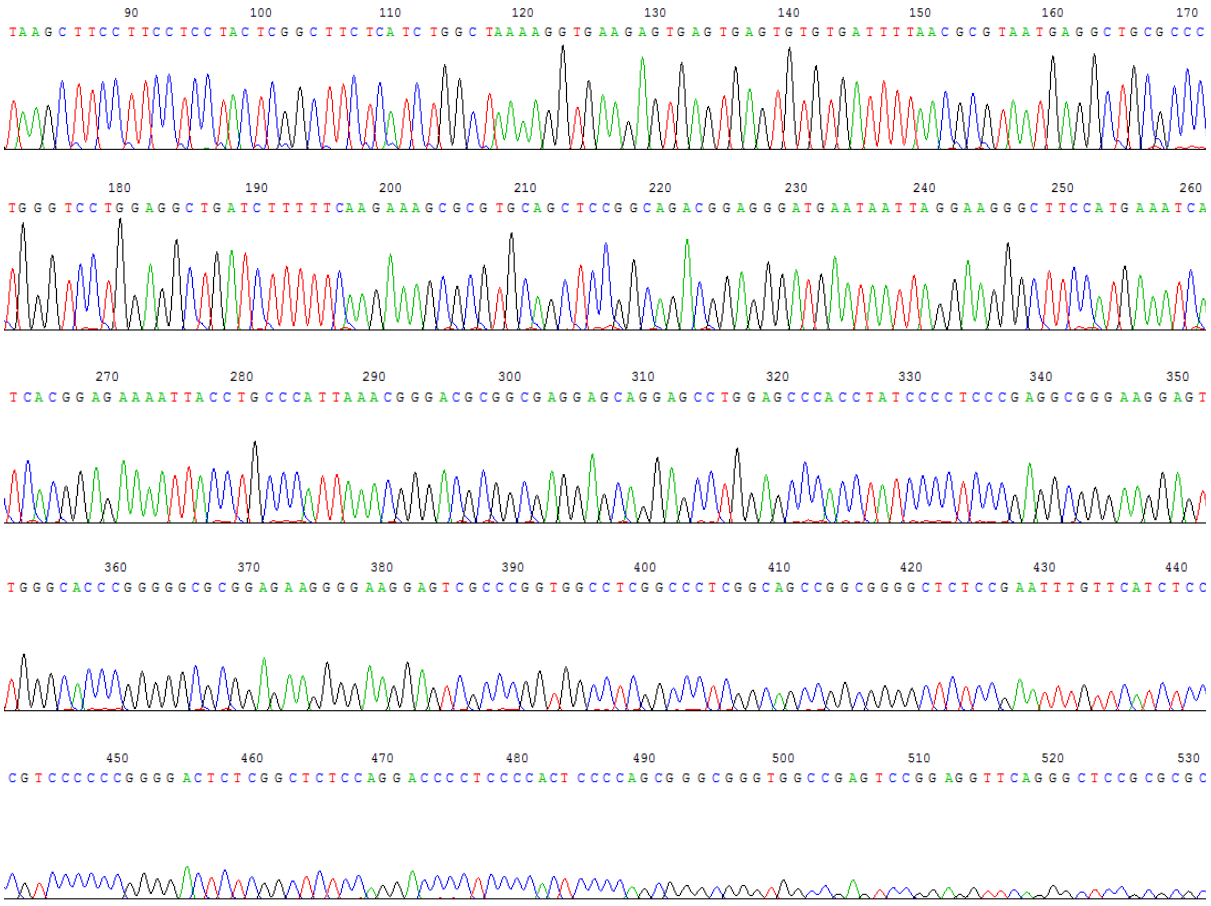

F1 Sequencing with GL2 Primer scans the region that resides between F4 and F3

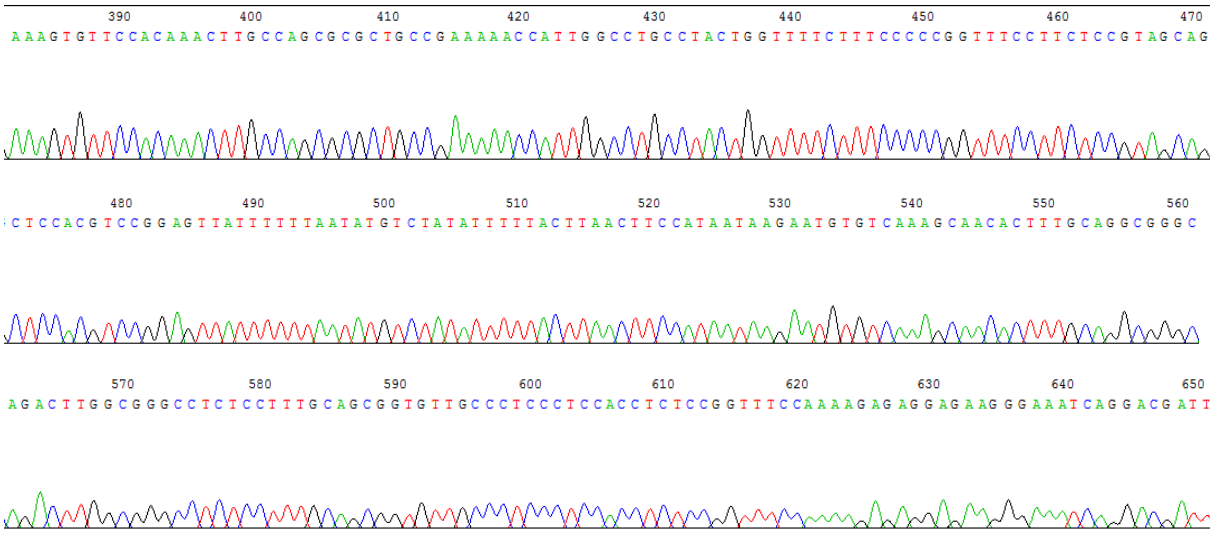

F1 sequencing with F4 primer which scans the last 600 bp of F1